Scaling in thermal convection: a unifying theory

By S I E G F R I E D G R O S S M A N N[1] AND D E T L E F L O H S E[2]

[1]Fachbereich Physik der Philipps-Universität Marburg, Renthof 6, D-35032 Marburg, Germany
e-mail: grossmann@physik.uni-marburg.de

[2]University of Twente, Department of Applied Physics, P.O. Box 217, 7500 AE Enschede,
The Netherlands
e-mail: lohse@tn.utwente.nl

A systematic theory for the scaling of the Nusselt number Nu and of the Reynolds number Re in strong Rayleigh–Bénard convection is suggested and shown to be compatible with recent experiments. It assumes a coherent large-scale convection roll ('wind of turbulence') and is based on the dynamical equations both in the bulk and in the boundary layers. Several regimes are identified in the Rayleigh number Ra versus Prandtl number Pr phase space, defined by whether the boundary layer or the bulk dominates the global kinetic and thermal dissipation, respectively, and by whether the thermal or the kinetic boundary layer is thicker. The crossover between the regimes is calculated. In the regime which has most frequently been studied in experiment ($Ra \lesssim 10^{11}$) the leading terms are $Nu \sim Ra^{1/4}Pr^{1/8}$, $Re \sim Ra^{1/2}Pr^{-3/4}$ for $Pr \lesssim 1$ and $Nu \sim Ra^{1/4}Pr^{-1/12}$, $Re \sim Ra^{1/2}Pr^{-5/6}$ for $Pr \gtrsim 1$. In most measurements these laws are modified by additive corrections from the neighbouring regimes so that the impression of a slightly larger (effective) Nu vs. Ra scaling exponent can arise. The most important of the neighbouring regimes towards large Ra are a regime with scaling $Nu \sim Ra^{1/2}Pr^{1/2}$, $Re \sim Ra^{1/2}Pr^{-1/2}$ for medium Pr ('Kraichnan regime'), a regime with scaling $Nu \sim Ra^{1/5}Pr^{1/5}$, $Re \sim Ra^{2/5}Pr^{-3/5}$ for small Pr, a regime with $Nu \sim Ra^{1/3}$, $Re \sim Ra^{4/9}Pr^{-2/3}$ for larger Pr, and a regime with scaling $Nu \sim Ra^{3/7}Pr^{-1/7}$, $Re \sim Ra^{4/7}Pr^{-6/7}$ for even larger Pr. In particular, a linear combination of the $\frac{1}{4}$ and the $\frac{1}{3}$ power laws for Nu with Ra, $Nu = 0.27Ra^{1/4} + 0.038Ra^{1/3}$ (the prefactors follow from experiment), mimics a $\frac{2}{7}$ power-law exponent in a regime as large as ten decades. For very large Ra the laminar shear boundary layer is speculated to break down through the non-normal-nonlinear transition to turbulence and another regime emerges. The theory presented is best summarized in the phase diagram figure 2 and in table 2.

1. Introduction

The early experiments on turbulent Rayleigh–Bénard (RB) convection in air cells with Prandtl number $Pr \approx 1$, summarized by Davis (1922*a,b*), showed a power-law increase of the Nusselt number Nu with the Rayleigh number Ra, namely, $Nu \sim Ra^{\gamma}$ with $\gamma = \frac{1}{4}$.† However, in these early experiments only relatively small Rayleigh numbers $Ra \lesssim 10^8$ were achieved. Later, when RB experiments with larger Rayleigh

† The symbol $\sim$ means 'scales as' throughout the text, *not* 'order of magnitude'. The prefactors are determined in §4.

numbers and in water cells with $Pr \approx 7$ were done, the power-law exponent γ turned out to be larger than $\frac{1}{4}$. The elegant theory of marginal stability by Malkus (1954), resulting in $\gamma = \frac{1}{3}$, seemed to describe those experiments.

In the late 1980s, Libchaber *et al.*'s experiments done at the University of Chicago on high Rayleigh number RB convection in a helium gas cell with Prandtl number $Pr \approx 1$ revealed new and unexpected scaling for the Nusselt number as a function of the Rayleigh number, namely $Nu \sim Ra^{\gamma}$ with $\gamma = 0.282 \pm 0.006$ (see Heslot, Castaing & Libchaber 1987; Castaing *et al.* 1989). The Reynolds number Re, characterizing the wind near the walls, i.e. the large-eddy mean flow, scaled as $Re \sim Ra^{\alpha}$ with $\alpha = 0.491 \pm 0.002$ (Castaing *et al.* 1989). These results were reproduced and extended in many experiments and numerical simulations, see Solomon & Gollub (1990), Wu & Libchaber (1991), Wu (1991), Procaccia *et al.* (1991), Werne (1993), Chilla *et al.* (1993), Siggia (1994), Cioni, Ciliberto & Sommeria (1995), Villermaux (1995), Kerr (1996), Shen, Tong & Xia (1996), Takeshita *et al.* (1996), Ciliberto, Cioni & Laroche (1996), Cioni, Ciliberto & Sommeria (1997), Xia & Lui (1997), Chavanne *et al.* (1997), Qiu & Xia (1998), Du & Tong (1998), Lui & Xia (1998), Benzi, Toschi & Tripiccione (1998); for review articles, which also summarize the results of earlier experimental, theoretical, and numerical work, we refer to Siggia (1994), Cioni *et al.* (1997), Zaleski (1998). From all these experiments at first sight it seems that at least the scaling exponent $\gamma \approx 0.282 \pm 0.006 \approx \frac{2}{7}$ is very robust.

Various theories were put forward to account for the scaling of the Nusselt number Nu and the Reynolds number Re as functions of the Rayleigh number Ra and the Prandtl number Pr. These include the Chicago mixing zone model (Castaing *et al.* 1989) and the theory by Shraiman & Siggia (1990), both reviewed in Siggia (1994), Cioni *et al.* (1997), Zaleski (1998). The main result of the Chicago model is $Nu \sim Ra^{2/7}$. The Chicago group did not focus on the Pr dependence as only experiments with $Pr \approx 1$ were done (Castaing *et al.* 1989). Later, Cioni *et al.* (1997) added the Pr dependence in the spirit of the Chicago model and obtained

$$Nu \sim Ra^{2/7} Pr^{2/7}, \qquad (1.1)$$

$$Re_{fluct} \sim Ra^{3/7} Pr^{-4/7}. \qquad (1.2)$$

Here, Re_{fluct} refers to the velocity *fluctuations* and not to the large-scale mean velocity (often denoted as the 'wind of turbulence') as Re does. This Prandtl number dependence is only expected to hold for $Pr < 1$ (Cioni *et al.* 1997; Zaleski 1998). On the other hand, the Shraiman–Siggia model, which assumes a turbulent boundary layer (BL) and a thermal boundary layer nested therein (i.e. Shraiman & Siggia implicitly assume a large enough Prandtl number), states

$$Nu \sim Ra^{2/7} Pr^{-1/7}, \qquad (1.3)$$

$$Re \sim Ra^{3/7} Pr^{-5/7} \quad \text{with logarithmic corrections.} \qquad (1.4)$$

For an extension of the Shraiman–Siggia theory to position-dependent shear rates see Ching (1997). The Prandtl number dependence of the Nusselt number resulting from the Castaing *et al.* (1989) model and from the theory by Shraiman & Siggia (1990) are not contradictory, as (1.1) has been suggested for small-Pr fluids and (1.3) for the large-Pr case. Indeed, in the large-Pr limit Zaleski (1998) derives the same Pr-dependence (1.3) as in the Shraiman–Siggia theory also from the Chicago model. However, both theories are based on rather different assumptions.

In recent years, the Prandtl number dependence of the Nusselt number has been measured and comparison with the theories by Castaing *et al.* (1989) and by Shraiman

& Siggia (1990) became possible. The first experiments were done with water and helium RB cells. However, comparing Nu in water and in helium convection only allows a small variation of the Prandtl number. From such experiments a small decrease of Nu with increasing Pr at given Ra was reported by Belmonte, Tilgner & Libchaber (1994): for $Ra = 10^9$ Belmonte *et al.* (1994) measured $Nu = 76 \pm 11$ for $Pr = 0.7$ and $Nu = 48 \pm 6$ for $Pr = 6.6$. Much larger Pr variations are possible if RB convection in mercury or liquid sodium is studied. Those experiments with a mercury RB cell ($Pr = 0.025$) by Rossby (1969), by Takeshita *et al.* (1996), and by Cioni *et al.* (1995, 1997) and with a liquid sodium RB cell ($Pr = 0.005$) by Horanyi, Krebs & Müller (1999) reveal that Nu *increases* with Pr, which is consistent with the Cioni *et al.* (1997) extension of the Chicago mixing zone model.

However, there seems to be indication that also the Chicago mixing zone model cannot account for all phenomena observed in recent experiments: one of the most startling observations is that there seems to be a small but significant trend of the scaling exponent γ as a function of Pr. For $Pr \approx 5$–7 (water) one has $\gamma = 0.28$–0.293 (Garon & Goldstein 1973; Tanaka & Miyata 1980; Siggia 1994; Lui & Xia 1998) for Ra up to $Ra \approx 10^9$ and an even larger $\gamma \approx \frac{1}{3}$ for larger $Ra \approx 10^9$–10^{11} (Goldstein & Tokuda 1980); for $Pr = 0.7$–1 (helium gas) it is $\gamma = 0.282 \pm 0.006$ (Castaing *et al.* 1989); for $Pr = 0.025$ (mercury) $\gamma = 0.247$ (Rossby 1969) and $\gamma = 0.26 \pm 0.02$ (Cioni *et al.* 1997) (for $Ra < 10^9$) have been measured; and for $Pr = 0.005$ (liquid sodium) it is $\gamma = 0.25$ (Horanyi, Krebs & Müller 1999). Those and further experimental results are summarized in table 1. Exponents between 0.25 and 0.33 have been measured! For thermal convection in a water RB cell ($Pr \approx 5$–7) with self-similarly distributed balls on the bottom wall, the scaling exponent can even be as large as $\gamma = 0.45$, presumably depending on the ball size distribution as found in Ciliberto & Laroche (1999).

Next, a *breakdown* of the $\gamma \approx \frac{2}{7}$ scaling regime at very large Ra has recently been observed, possibly towards a scaling regime $Nu \sim Ra^{1/2}$, which had been predicted by Kraichnan (1962) decades ago. For $Pr = 0.025$ Cioni *et al.* (1997) saw the breakdown at $Ra \sim 2 \times 10^9$ (and a startling small window with a local scaling exponent smaller than $\frac{2}{7}$ for $Ra \sim 5 \times 10^8$–2×10^9) while for $Pr = 0.7$–1.0 Chavanne *et al.* (1997) observed it at $Ra \sim 10^{11}$. The transition around $Ra \approx 10^{11}$ in figure 3 of Siggia (1994), showing $Nu/Ra^{2/7}$ vs. Ra from the data by Wu (1991), may already be interpreted as the same breakdown. On the other hand, Glazier *et al.* (1999) did not observe such a transition. Thus, the experimental situation itself is not yet clear.

All these observations and also the more intuitive rather than equation of motion based approach of Castaing *et al.* (1989) call for a re-examination and extension of the existing scaling theories for thermal convection. Of course, a mathematically rigorous derivation of $Nu(Ra, Pr)$ and $Re(Ra, Pr)$ is hardly possible. The known rigorous bounds overestimate the measured Nusselt numbers by more than one order of magnitude and are only able to give the scaling exponent of the Kraichnan regime $\gamma = \frac{1}{2}$, see Howard (1972), Busse (1978), Doering & Constantin (1996).

Though without a strict mathematical derivation, the guideline of the presented approach will be the dynamical equations for the velocity field $u(x, t)$, the kinematic pressure field $p(x, t)$, and the temperature field $\theta(x, t)$,

$$\partial_t u_i + u_j \partial_j u_i = -\partial_i p + \nu \partial_j^2 u_i + \beta g \delta_{i3} \theta, \tag{1.5}$$

$$\partial_t \theta + u_j \partial_j \theta = \kappa \partial_j^2 \theta, \tag{1.6}$$

assisted by the appropriate boundary conditions at the bottom wall $z = 0$, the top wall $z = L$, and the sidewalls of the cell. Here, g is the gravitational acceleration, β

Reference	fluid	Pr	Ra range	γ
Ashkenazi & Steinberg (1999)	SF_6	1–93	10^9–10^{14}	0.30 ± 0.03
Garon & Goldstein (1973)	H_2O	5.5	10^7–3×10^9	0.293
Tanaka & Miyata (1980)	H_2O	6.8	3×10^7–4×10^9	0.290
Goldstein & Tokuda (1980)	H_2O	6.5	10^9–2×10^{11}	$\frac{1}{3}$
Qiu & Xia (1998)	H_2O	≈ 7	2×10^8–2×10^{10}	0.28
Lui & Xia (1998)	H_2O	≈ 7	2×10^8–2×10^{10}	0.28 ± 0.06
Shen *et al.* (1996)	H_2O	≈ 7	8×10^7–7×10^9	0.281 ± 0.015
Threlfall (1975)	He	0.8	4×10^5–2×10^9	0.280
Castaing *et al.* (1989)	He	0.7–1	$\lesssim 10^{11}$	0.282 ± 0.006
Wu & Libchaber (1991)	He	0.6–1.2	4×10^7–10^{12}	0.285
Chavanne *et al.* (1997)	He	0.6–0.73	3×10^7–10^{11}	$\frac{2}{7}$
Davis (1922)	air	≈ 1	$\lesssim 10^8$	0.25
Rossby (1969)	Hg	0.025	2×10^4–5×10^5	0.247
Takeshita *et al.* (1996)	Hg	0.025	10^6–10^8	0.27
Cioni *et al.* (1997)	Hg	0.025	5×10^6–5×10^8	0.26 ± 0.02
Cioni *et al.* (1997)	Hg	0.025	4×10^8–2×10^9	0.20
Glazier *et al.* (1999)	Hg	0.025	2×10^5–8×10^{10}	0.29 ± 0.01
Horanyi *et al.* (1998)	Na	0.005	$\lesssim 10^6$	0.25

TABLE 1. Power-law exponents γ of the power law $Nu \sim Ra^{\gamma}$ for various experiments. The experiments were done with different aspect ratios; however, no strong dependence of the scaling exponent γ on the aspect ratio is expected (in contrast to the prefactors, which do have an aspect ratio dependence as found by Wu & Libchaber 1992).

the isobaric thermal expansion coefficient, ν the kinematic viscosity, κ the thermal diffusivity, and L the height of the RB cell; the temperature difference between top and bottom walls is called Δ.

The second feature of our approach introduced in §2 is that we try to be as systematic as possible. We will be able to identify four different main scaling regimes for Re and Nu in the Ra, Pr phase space, depending on whether the BL or the bulk dominates the *global* thermal and kinetic energy dissipation, respectively. Three of the four regimes consist of two subregimes, depending on whether the thermal BL or the viscous BL is thicker. We also calculate the validity range of the scaling laws and make predictions on the stability of the different regimes. In §3 we compare the power-law exponents of the theory with experimental data. In §4 we try to adopt the prefactors of the theory from some experimental information and compare the resulting prefactors to further experiments. Section 5 contains a summary and conclusions.

2. Boundary layer vs. bulk dominance of kinetic and thermal dissipation
2.1. *Definitions*

The parameter space of RB convection is spanned by the Rayleigh and Prandtl numbers,

$$Ra = \frac{\beta g L^3 \Delta}{\kappa \nu}, \qquad Pr = \frac{\nu}{\kappa}. \tag{2.1}$$

Our main focus is on the resulting Reynolds and Nusselt numbers,

$$Re = \frac{UL}{\nu}, \qquad Nu = \frac{\langle u_z \theta \rangle_A - \kappa \partial_3 \langle \theta \rangle_A}{\kappa \Delta L^{-1}}, \tag{2.2}$$

where $\langle . \rangle_A$ denotes the average over (any) z-plane. Correspondingly, $\langle . \rangle_V$ used below denotes the volume average. U is the mean large-scale velocity near the boundaries of the cell. It is the remainder of the convection rolls which in the turbulent regime manifests itself as coherent large-scale convection flow, as first discovered by Krishnamurti & Howard (1981) and later found by various groups (see Zocchi, Moses & Libchaber 1990; Wu 1991; Castaing *et al.* 1989; Belmonte, Tilgner & Libchaber 1993, 1994; Tilgner, Belmonte & Libchaber 1993; Siggia 1994; Xin, Xia & Tong 1996; Qui & Xia 1998). The existence of this 'wind of turbulence' is one of the central assumptions of our theory. We consider this to be a weak assumption, given the overwhelming experimental evidence. The effect of the wind is twofold: (i) in the region between the wind and the cell wall a shear flow boundary layer will build up; (ii) the wind stirs the fluid in the bulk. In the presented theory we consider the velocity fluctuations in the bulk of the cell only as a consequence of the stirring by the large-scale roll. Therefore, the Reynolds number Re based on the roll velocity rather than the one based on the fluctuations Re_{fluct} in the bulk is taken as the more appropriate to theoretically describe the bulk turbulence. Though the theory assumes the existence of the large-scale wind, it does not make any statement on how the large-scale wind contributes to the heat transport. There is experimental evidence by Ciliberto *et al.* (1996) that it hardly does.

2.2. *Decomposition of the energy dissipation*

The starting points of the present theory are the kinetic and thermal dissipation rates

$$\epsilon_u(\boldsymbol{x}, t) = \nu(\partial_i u_j(\boldsymbol{x}, t))^2, \tag{2.3}$$

$$\epsilon_\theta(\boldsymbol{x}, t) = \kappa(\partial_i \theta(\boldsymbol{x}, t))^2. \tag{2.4}$$

Their *global averages* $\langle \epsilon_u(\boldsymbol{x}, t) \rangle_V = \epsilon_u$ and $\langle \epsilon_\theta(\boldsymbol{x}, t) \rangle_V = \epsilon_\theta$ obey the following rigorous relations, which are easily derivable from the equations of motion, see e.g. Shraiman & Siggia (1990), Siggia (1994):

$$\epsilon_u = \frac{\nu^3}{L^4}(Nu - 1)Ra Pr^{-2}, \tag{2.5}$$

$$\epsilon_\theta = \kappa \frac{\Delta^2}{L^2} Nu. \tag{2.6}$$

Dissipation takes place both in the bulk of the flow and in the boundary layers. Near the walls thermal and kinetic boundary layers of thicknesses λ_θ and λ_u develop, which are determined by the thermal diffusivity κ and the kinematic viscosity ν, respectively, and which are in general different, depending on Pr. They are defined on the basis of the temperature and of the velocity profiles, respectively. Whenever there exists a thermal shortcut in the bulk due to the turbulent convective transport, the width of the thermal boundary layer is connected with the Nusselt number by

$$\lambda_\theta = \tfrac{1}{2}L Nu^{-1}. \tag{2.7}$$

The thickness of the kinetic boundary layer can be expressed in terms of the Reynolds number,

$$\lambda_u \sim L Re^{-1/2}. \tag{2.8}$$

Here, we have assumed that there is laminar viscous flow of Blasius type (cf. §§ 39 and 41 of Landau & Lifshitz 1987) in the boundary layer; the lateral extent x of the BL has been identified with the height L of the cell, reflecting that the wind organizes in

the form of a large-scale roll. The transition to turbulence in the boundary layers will be considered in §2.6. Though for large enough Ra the total volume of the BLs is rather small, their contribution to the global average dissipation may be considerable, as the velocity and the temperature gradients in the BLs are much larger than in the bulk.

In general, we decompose the globally averaged dissipation rates into their BL and bulk contributions,

$$\epsilon_u = \epsilon_{u,BL} + \epsilon_{u,bulk}, \qquad (2.9)$$

$$\epsilon_\theta = \epsilon_{\theta,BL} + \epsilon_{\theta,bulk}, \qquad (2.10)$$

where

$$\epsilon_{u,BL} = \int_{0 \leqslant z \leqslant \lambda_u} + \int_{L-\lambda_u \leqslant z \leqslant L} \mathrm{d}z \, v (\partial_i u_j)^2 / L = v \left\langle (\partial_i u_j (\boldsymbol{x} \in BL, t))^2 \right\rangle_V$$

is the viscous dissipation taking place in the viscous BL,

$$\epsilon_{\theta,BL} = \int_{0 \leqslant z \leqslant \lambda_\theta} + \int_{L-\lambda_\theta \leqslant z \leqslant L} \mathrm{d}z \, \kappa (\partial_i \theta)^2 / L = \kappa \left\langle (\partial_i \theta (\boldsymbol{x} \in BL, t))^2 \right\rangle_V$$

is the thermal dissipation taking place in the thermal BL,

$$\epsilon_{u,bulk} = \int_{\lambda_u \leqslant z \leqslant L-\lambda_u} \mathrm{d}z \, v (\partial_i u_j)^2 / L = v \left\langle (\partial_i u_j (\boldsymbol{x} \in bulk, t))^2 \right\rangle_V$$

is the viscous dissipation taking place in the bulk, etc.

This kind of thinking immediately suggests the existence of four regimes:

(*I*) both ϵ_u and ϵ_θ are dominated by their BL contributions;

(*II*) ϵ_θ is dominated by $\epsilon_{\theta,BL}$ and ϵ_u is dominated by $\epsilon_{u,bulk}$;

(*III*) ϵ_u is dominated by $\epsilon_{u,BL}$ and ϵ_θ is dominated by $\epsilon_{\theta,bulk}$;

(*IV*) both ϵ_u and ϵ_θ are bulk dominated.

For (relatively) small Ra the BLs are thickest, therefore regime I is expected. On the other hand, for large Ra the BLs are very thin and we will expect regime IV, provided that the volume reduction of the BL is more efficient than the dissipation increase in the BLs due to the growing shear rate. Next, for small Pr the viscous BL is smaller than the thermal one, $\lambda_u \ll \lambda_\theta$, and we expect regime II. Finally, for large Pr it is $\lambda_u \gg \lambda_\theta$ and we have regime III.

A priori it is not clear whether all four regimes can exist. However, after input of some experimental information, we will see that they are likely to exist. We will also calculate the scaling of the borders between the different regimes in the Ra, Pr phase space. Of course, these lines do not indicate sharp transitions but the range of the change of dominance.

2.3. *Estimate of bulk and BL contributions*

The next step is to estimate the various contributions $\epsilon_{u,BL}$, $\epsilon_{\theta,BL}$, $\epsilon_{u,bulk}$, $\epsilon_{\theta,bulk}$ of the BL and the bulk dissipation from the dynamical equations (1.5) and (1.6), expressing them as functions of Nu, Re, Ra, and Pr.

Bulk contributions

We start with the *kinetic dissipation*. As already outlined above, the theory assumes that the bulk fluctuations with typical velocity u_{fluct} originate from the large-scale coherent flow with velocity U. If there is no such 'wind of turbulence', the following

estimates cease to be valid; even the Reynolds number $Re = UL/v$ cannot be defined properly. Clearly, this will happen in the regime of very large Prandtl numbers where the flow is suppressed by the strong viscosity. Therefore, there will be a transition line $Pr(Ra)$ in phase space, defined by, say, $Re = 50$, beyond which the theory no longer holds; we will calculate this line in §2.5. Another limit of applicability is in the very small-Pr range. Here, κ is so large that the heat is molecularly conducted, thus $Nu = 1$. Other possible limitations of the basic assumptions of the theory will be discussed in §5.

The assumption of the large-scale velocity U stirring the bulk implies the picture of a turbulent energy cascade in the bulk which in turn suggests how to estimate the *bulk* dissipation rates, namely by balancing the dissipation with the large-scale convective term in the energy equation following from (1.5),

$$\epsilon_{u,bulk} = v \left\langle (\partial_i u_j (\boldsymbol{x} \in bulk, t))^2 \right\rangle_V \sim \frac{U^3}{L} = \frac{v^3}{L^4} Re^3. \qquad (2.11)$$

As argued before, we took as the relevant velocity scale the wind velocity U and not the velocity fluctuations u_{fluct} because it is U which stirs the fluid in the bulk. This is a key assumption of the theory, justified by intuition and by the results. The theory presented does not make any statement on the Ra-scaling of the typical bulk fluctuations u_{fluct}.

We explicitly remark that the findings on the Re dependence of the energy dissipation rate in Taylor–Couette flow by Lathrop, Fineberg & Swinney (1992) do not contradict (2.11). Lathrop *et al.* (1992) found that $\epsilon_u L^4 v^{-3} Re^{-3}$ still depends on Re even for large Re. However, their result refers to the global ϵ_u, not to $\epsilon_{u,bulk}$. Possible intermittency corrections are not taken into consideration in (2.11) as they are at most small (see Grossmann 1995).

We note that strictly speaking there should be a factor $(L - 2\lambda_u)/L$ on the right-hand side of (2.11), as the average $\epsilon_{u,bulk} = \langle \epsilon_u(\boldsymbol{x} \in bulk, t) \rangle_V$ refers to the whole volume. However, it is assumed that the state is already turbulent enough, i.e. Ra large enough, so that $\lambda_u \ll L$. The validity of this assumption limits the scaling ranges to be derived.

The estimate of the *thermal* bulk dissipation $\epsilon_{\theta,bulk}$ is slightly more complicated, as the velocity field $\boldsymbol{u}(\boldsymbol{x}, t)$ matters in the dynamical equation (1.6) for the temperature. In particular, it matters whether the kinetic BL, characterized by a linear velocity profile, is nested in the thermal one or if it is the other way round.

For the former case ($\lambda_u < \lambda_\theta$, i.e. small Pr, see figure 1a) the thermal boundary layer can be estimated in complete analogy to (2.11) as

$$\epsilon_{\theta,bulk} = \kappa \left\langle (\partial_i \theta (\boldsymbol{x} \in bulk, t))^2 \right\rangle_V \sim \frac{U\Delta^2}{L} = \kappa \frac{\Delta^2}{L^2} Pr Re. \qquad (2.12)$$

Note that corresponding to U in (2.11) we took the large-scale temperature difference Δ in (2.12), not the typical temperature fluctuations Δ_{fluct}. Again, this is a key assumption, justified by the later results.

For the latter case ($\lambda_u > \lambda_\theta$, i.e. large Pr, see figure 1b) we must realize that at the merging of the (linear) thermal BL into the thermal bulk the velocity is not U itself, but smaller by a factor $\lambda_\theta / \lambda_u < 1$. Therefore, it is reasonable to assume that $U\lambda_\theta / \lambda_u$ is the relevant velocity for the estimate of $\epsilon_{\theta,bulk}$, i.e.

$$\epsilon_{\theta,bulk} \sim \frac{\lambda_\theta}{\lambda_u} \frac{U\Delta^2}{L} = \kappa \frac{\Delta^2}{L^2} Pr Re^{3/2} Nu^{-1}. \qquad (2.13)$$
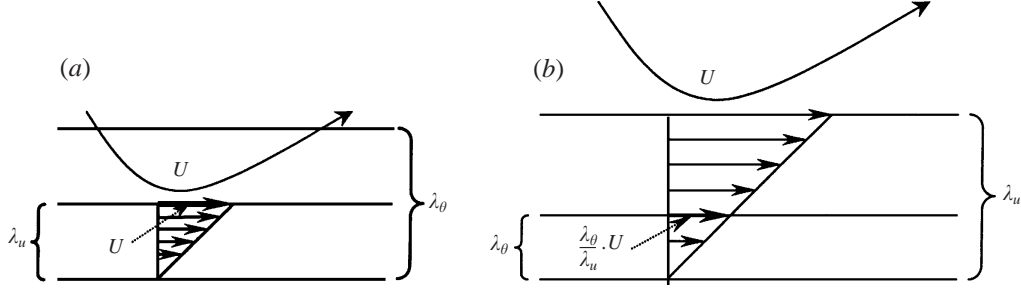
FIGURE 1. Sketch of the boundary layers, (*a*) for low *Pr* where $\lambda_u < \lambda_\theta$
and (*b*) for large *Pr* where $\lambda_u > \lambda_\theta$.

BL contributions

For $\epsilon_{u,BL}$ we follow an idea by Chavanne *et al.* (1997) and estimate, using (2.8),

$$\epsilon_{u,BL} = \nu \left\langle (\partial_i u_j(\boldsymbol{x} \in BL, t))^2 \right\rangle_V \sim \nu \frac{U^2}{\lambda_u^2} \frac{\lambda_u}{L} \sim \frac{\nu^3}{L^4} Re^{5/2}. \tag{2.14}$$

Here, U/λ_u characterizes the order of magnitude of $\partial_i u_j$ and the factor λ_u/L accounts for the BL fraction of the total volume. Again, this reasoning breaks down when there is no large-scale 'wind of turbulence'. Correspondingly, we estimate

$$\epsilon_{\theta,BL} = \kappa \left\langle (\partial_i \theta(\boldsymbol{x} \in BL, t))^2 \right\rangle_V \sim \kappa \frac{\Delta^2}{\lambda_\theta^2} \frac{\lambda_\theta}{L} \sim \kappa \frac{\Delta^2}{L^2} Nu. \tag{2.15}$$

Equations (2.11) to (2.15) express the various dissipation contributions (and thus the total dissipations ϵ_u and ϵ_θ, (2.9) and (2.10)) in terms of *Ra*, *Pr*, *Re*, and *Nu*. If we insert (2.11) to (2.15) into the rigorous relations (2.5) and (2.6), we obtain two equations, allowing *Nu* and *Re* to be expressed in terms of *Ra* and *Pr*. If we only take the dominating contributions ϵ_{BL} or ϵ_{bulk} in ϵ_u and ϵ_θ, respectively, the formulae for the four regimes *I*, *II*, *III*, and *IV* are obtained, describing pure scaling instead of superpositions.

With this idea in mind, the scaling of the thermal boundary layer dissipation (2.15), though correct, does not give new information. It coincides with the rigorous relation (2.6). The physical reason is that the bulk is considered to provide a thermal shortcut. Therefore, we make use of the dynamics in the thermal BL in more detail. We approximate (systematically in order $1/Re$) (1.6) by the dominant terms (cf. Landau & Lifshitz 1987 or Shraiman & Siggia 1990; Cioni *et al.* 1997)

$$u_x \partial_x \theta + u_z \partial_z \theta = \kappa \partial_z^2 \theta \tag{2.16}$$

in the thermal BL. Both terms on the left-hand side are of the same order of magnitude as can be concluded from the incompressibility condition $\partial_x u_x + \partial_z u_z \approx 0$. In the lower subregimes with $\lambda_u < \lambda_\theta$ the velocity u_x must be estimated by U, in the upper subregimes with $\lambda_u > \lambda_\theta$ it is as argued above $u_x \sim U\lambda_\theta/\lambda_u$, see figure 1. In addition, $\partial_x \sim 1/L$ and $\kappa\partial_z^2 \sim \kappa/\lambda_\theta^2$. Therefore, for $\lambda_u < \lambda_\theta$ we finally get

$$Nu \sim Re^{1/2} Pr^{1/2} \tag{2.17}$$

and for $\lambda_u > \lambda_\theta$ we have

$$Nu \sim Re^{1/2} Pr^{1/3}. \tag{2.18}$$

Equations (2.17) and (2.18) replace the correct (but useless) relation $\epsilon_\theta \sim \epsilon_{\theta,BL}$ which does not add new information beyond (2.6).

2.4. *Four regimes*

We will start with the $\epsilon_{\theta,bulk}$ dominated regimes (III and IV).

Regime IV, $\epsilon_u \sim \epsilon_{u,bulk}$ and $\epsilon_\theta \sim \epsilon_{\theta,bulk}$ (large Ra)

Depending on whether λ_u is less or larger than λ_θ we must use (2.12) or (2.13), respectively, for the $\epsilon_{\theta,bulk}$ estimate. The former happens for low Pr, the latter for large Pr. Therefore, we will give these two subregimes the index l for lower and u for upper. At which line $Pr(Ra)$ in phase space $\lambda_u = \lambda_\theta$ the crossover from the $\lambda_u < \lambda_\theta$ to the $\lambda_u > \lambda_\theta$ will occur is not clear *a priori*. We will calculate this line $\lambda_u = \lambda_\theta$ later with additional experimental information.

In regime IV_l we use (2.11) for ϵ_u in (2.5) and (2.12) for ϵ_θ in (2.6) to obtain

$$Nu \sim Ra^{1/2}Pr^{1/2}, \tag{2.19}$$

$$Re \sim Ra^{1/2}Pr^{-1/2}. \tag{2.20}$$

We recognize the asymptotic Kraichnan regime (Kraichnan 1962), just as expected for large Ra when both thermal and kinetic energy dissipation are bulk dominated. Note that other lines of arguments can also lead to (2.19), see e.g. Kraichnan's work itself (Kraichnan 1962), Spiegel (1971), or our reasoning in §2.6. Therefore, (2.19) seems to be quite robust. The physics of this regime is that the dimensional heat current $Nu\kappa\Delta/L$ is independent of both κ and v.

In regime IV_u we substitute as before (2.11) for ϵ_u into (2.5) but now (2.13) instead of (2.12) for ϵ_θ into (2.6) to obtain

$$Nu \sim Ra^{1/3}, \tag{2.21}$$

$$Re \sim Ra^{4/9}Pr^{-2/3}. \tag{2.22}$$

The Nu scaling is the one also following from the theory by Malkus (1954).

Regime III, $\epsilon_u \sim \epsilon_{u,BL}$ and $\epsilon_\theta \sim \epsilon_{\theta,bulk}$ (large Pr)

Again we have to distinguish between the lower subregime III_l with $\lambda_u < \lambda_\theta$ and the upper one III_u with $\lambda_u > \lambda_\theta$. For III_l we combine (2.14) with (2.5) and (2.12) with (2.6) and get

$$Nu \sim Ra^{2/3}Pr^{1/3}, \tag{2.23}$$

$$Re \sim Ra^{2/3}Pr^{-2/3}. \tag{2.24}$$

This regime will turn out to be small and less important. The more important one is III_u: combine (2.14) with (2.5) and (2.13) with (2.6) to obtain

$$Nu \sim Ra^{3/7}Pr^{-1/7}, \tag{2.25}$$

$$Re \sim Ra^{4/7}Pr^{-6/7}. \tag{2.26}$$

This regime may be observable for large enough Pr when $\lambda_u \gg \lambda_\theta$. To our knowledge to date this regime has neither been observed nor predicted.

Later, we will find hints of this regime III_u in the form of a subleading correction to describe the data by Chavanne *et al.* (1997). It would be nice to perform further experiments with large Pr to be able to more cleanly identify this postulated regime III_u. We note that it is not in contradiction with the upper estimate by Chan

(1971), $Nu \leqslant \text{const} Ra^{1/3}$, holding in the infinite-Pr limit (for fixed Ra), and also not in contradiction with the rigorous upper bound by Constantin & Doering (1999) $Nu \leqslant \text{const} Ra^{1/3}(1+\log Ra)^{2/3}$, holding in the same $Pr \to \infty$ limit. The reason is that regime III_u is for finite Pr; if $Pr \to \infty$, then $Ra \to \infty$ also, if one wants to stay in regime III_u.

Regime II, $\epsilon_u \sim \epsilon_{u,bulk}$ and $\epsilon_\theta \sim \epsilon_{\theta,BL}$ (small Pr)

Regime II_l: Combining (2.11) with (2.5) gives together with (2.17)

$$Nu \sim Ra^{1/5} Pr^{1/5}, \qquad (2.27)$$

$$Re \sim Ra^{2/5} Pr^{-3/5}. \qquad (2.28)$$

This regime should appear for small enough Pr when $\lambda_u \ll \lambda_\theta$. Indeed, Cioni *et al.* (1997) observed experimental hints of such a regime; also (2.27)–(2.28) have already been derived by them in a similar way. A power law $Nu \sim Ra^{1/5}$ has already been suggested by Roberts (1979).

Regime II_u: Because of the two competing conditions $\epsilon_\theta \sim \epsilon_{\theta,BL}$ (i.e. Pr small) and $\lambda_u > \lambda_\theta$ (i.e. Pr large) such a subregime can at most be small. It will turn out later that it will probably not exist at all. Nevertheless, for completeness we give the scaling laws, resulting from now taking (2.18) and, as before, inserting (2.11) into (2.5), namely

$$Nu \sim Ra^{1/5}, \qquad (2.29)$$

$$Re \sim Ra^{2/5} Pr^{-2/3}. \qquad (2.30)$$

Regime I, $\epsilon_u \sim \epsilon_{u,BL}$ and $\epsilon_\theta \sim \epsilon_{\theta,BL}$

Regime I_l: This is the regime of (comparatively) small Ra whose scaling we obtain from using (2.17) and substituting (2.14) for ϵ_u in (2.5), namely

$$Nu \sim Ra^{1/4} Pr^{1/8}, \qquad (2.31)$$

$$Re \sim Ra^{1/2} Pr^{-3/4}. \qquad (2.32)$$

We argue that this is the regime whose scaling behaviour has been observed in almost all thermal turbulence experiments (see Heslot *et al.* 1987; Castaing *et al.* 1989; Solomon & Gollub 1990; Wu & Libchaber 1991; Wu 1991; Procaccia *et al.* 1991; Chilla *et al.* 1993; Siggia 1994; Cioni *et al.* 1995, 1997; Takeshita *et al.* 1996; Ciliberto *et al.* 1996; Xin *et al.* 1996; Xia & Lui 1997; Chavanne *et al.* 1997; Qiu & Xia 1998; Lui & Xia 1998), but that in nearly all cases the pure scaling behaviour (2.31) and (2.32) has been polluted by sub-dominant contributions from the neighbouring regimes, as we will elaborate in detail in the next section.

Remarkably, it is this power law $Nu \sim Ra^{1/4}$ which was the first one suggested by Davis (1922*a, b*) and which has been well known in the engineering literature for a long time, see Faber (1995). It also holds for two-dimensional convection in the low Prandtl number limit, as shown by Clever & Busse (1981) and Busse & Clever (1981).

Regime I_u: The scaling in I_u is obtained from equation (2.18) and combining (2.14) with (2.5), namely

$$Nu \sim Ra^{1/4} Pr^{-1/12}, \qquad (2.33)$$

$$Re \sim Ra^{1/2} Pr^{-5/6}. \qquad (2.34)$$

Note that the Ra dependence is the same as in I_l, but now Nu decreases with increasing Pr. This behaviour is physically to be expected because due to increasing ν

the convective heat transport is more and more reduced. And indeed, such a crossover from increase to decrease of Nu with Pr has been observed in experiment. It will later give us the opportunity to determine the transition line $\lambda_u = \lambda_\theta$.

The scaling of this crossover line can be determined here from equating $\lambda_\theta \sim L/Nu$ and $\lambda_u \sim L/\sqrt{Re}$ in the respective regimes. We obtain

$$Pr_\lambda^{I_l - I_u} \sim Ra^0, \tag{2.35}$$

$$Pr_\lambda^{II_l - II_u} \sim Ra^0, \tag{2.36}$$

$$Pr_\lambda^{III_l - III_u} \sim Ra^{-1/2}, \tag{2.37}$$

$$Pr_\lambda^{IV_l - IV_u} \sim Ra^{-1/3}. \tag{2.38}$$

Because the line $\lambda_u = \lambda_\theta$ obeys $Pr = \mathrm{const}$ in regime I it is either above or below the common corner point of all four regimes. Therefore it can go either through regime III or through regime II, but not through both. Thus either regime II_u will exist or regime III_l, never both of them.

We now calculate the scaling of the boundaries between the other different domains in the Ra, Pr phase space. The boundary between I and II is obtained by equating $\epsilon_{u,BL} \sim \epsilon_{u,bulk}$, that between I and III by equating $\epsilon_{\theta,BL} \sim \epsilon_{\theta,bulk}$, etc. The results are

$$Pr_{trans}^{I_l - II_l} \sim Ra_{trans}^{2/3}, \tag{2.39}$$

$$Pr_{trans}^{I_l - III_l} \sim Ra_{trans}^{-2}, \tag{2.40}$$

$$Pr_{trans}^{III_l - IV_l} \sim Ra_{trans}^{1}, \tag{2.41}$$

$$Pr_{trans}^{II_l - IV_l} \sim Ra_{trans}^{-1}, \tag{2.42}$$

$$Pr_{trans}^{I_u - III_u} \sim Ra_{trans}^{3}, \tag{2.43}$$

$$Pr_{trans}^{III_u - IV_u} \sim Ra_{trans}^{2/3}. \tag{2.44}$$

Note that all these lines indicate the range of smooth crossover in the dominance of either the BL or the bulk dissipation.

The phase diagram in Ra, Pr phase space with the various regimes and crossovers is shown in figure 2, anticipating the prefactors of the power laws, whose exponents we have evaluated up to now. We will determine the prefactors in (2.17)–(2.44) in §4 from four pieces of experimental information. This experimental information all comes from experiments with an aspect ratio of the RB cell of the order of 1. Based on the work by Wu & Libchaber 1992, we expect the prefactors to depend on the aspect ratio; therefore, all prefactors given in this paper only refer to aspect ratio order of 1 experiments.

2.5. *Range of validity of power laws*

What is the range of validity of the power laws summarized in table 2? For too small Reynolds numbers towards larger Pr, say, $Re_{crit} = 50$, the distinction between the bulk and the boundary layer is no longer meaningful; the bulk will no longer be driven to turbulence by a large-scale velocity U. Correspondingly, if the Nusselt number approaches 1 because of too small Pr, the splitting of ϵ_θ in $\epsilon_{\theta,BL}$ and $\epsilon_{\theta,bulk}$ becomes meaningless. Finally, for $Nu = 1$, we no longer have thermal convection but pure thermal diffusion.

Therefore, we impose the restrictions $Re \lesssim 50$ towards large Pr and $Nu \gtrsim 1$ towards small Pr. The lines $Re = 50$ and $Nu = 1$ are included in the phase diagram
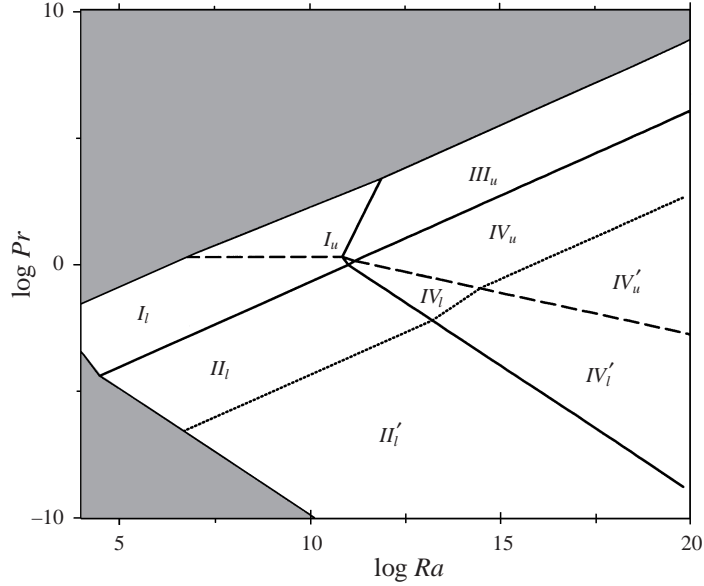
FIGURE 2. Phase diagram in the (Ra, Pr)-plane. The power laws and the corresponding prefactors (to be determined in §4) in the respective regimes are summarized in table 2. The tiny regime to the right of regime I_l is regime III_l. The dashed line is $\lambda_u = \lambda_\theta$. The shaded regime for large Pr is where $Re \leqslant 50$, and in the shaded regime for low Pr we have $Nu = 1$. The dotted line indicates the non-normal-nonlinear onset of turbulence in the BL shear flow discussed in §2.6. The scaling in regime II_l' is therefore as in the bulk-dominated regime IV_l. The power laws for the boundaries between the different regimes are given in table 3.

figure 2. Their analytical forms directly follow from the power laws of table 2; they are given in table 3.

Beyond these lines, in the shaded areas in figure 2, the flow is viscosity dominated or thermal diffusivity dominated and the proposed power laws for Re and Nu (table 2) no longer apply.

2.6. *Turbulence transition of the laminar boundary layer*

For very large Ra the theory outlined here requires an extension. It is based so far on the existence of a laminar boundary layer flow of Blasius type; its thickness therefore obeys $\lambda_u \sim L Re^{-1/2}$, cf. §39 of Landau & Lifshitz (1987). The shear in this boundary layer is determined by the large-scale velocity U of the thermal rolls in the RB cell and the boundary layer width λ_u. We define the corresponding shear Reynolds number as

$$Re_{shear} = \frac{U\lambda_u}{\nu} \sim \sqrt{Re}. \qquad (2.45)$$

The key issue now is that the laminar shear BL will become turbulent for large enough Re_{shear}. The details of the mechanism of this turbulence transition are still under study but it seems to have *non-normal-nonlinear* features (see Drazin & Reid 1981; Boberg & Brosa 1988; Trefethen *et al.* 1993; Gebhardt & Grossman 1994; Waleffe 1995; Schmiegel & Eckhardt 1997; Grossmann 1999). What however is agreed upon is that the shear Reynolds number at which the turbulence sets in depends on the kind and strength of the flow distortion. A typical value for the onset is (see Landau & Lifshitz 1987)

$$Re_{shear,turb} = 420. \qquad (2.46)$$

Regime	Dominance of	BL	Nu	Re
I_l	$\epsilon_{u,BL}$, $\epsilon_{\theta,BL}$	$\lambda_u < \lambda_\theta$	$0.27 Ra^{1/4} Pr^{1/8}$	$0.037 Ra^{1/2} Pr^{-3/4}$
I_u		$\lambda_u > \lambda_\theta$	$0.33 Ra^{1/4} Pr^{-1/12}$	$0.039 Ra^{1/2} Pr^{-5/6}$
II_l	$\epsilon_{u,bulk}$, $\epsilon_{\theta,BL}$	$\lambda_u < \lambda_\theta$	$0.97 Ra^{1/5} Pr^{1/5}$	$0.47 Ra^{2/5} Pr^{-3/5}$
(II_u)		$\lambda_u > \lambda_\theta$	$(\sim Ra^{1/5})$	$(\sim Ra^{2/5} Pr^{-2/3})$
III_l	$\epsilon_{u,BL}$, $\epsilon_{\theta,bulk}$	$\lambda_u < \lambda_\theta$	$6.43 \times 10^{-6} Ra^{2/3} Pr^{1/3}$	$5.24 \times 10^{-4} Ra^{2/3} Pr^{-2/3}$
III_u		$\lambda_u > \lambda_\theta$	$3.43 \times 10^{-3} Ra^{3/7} Pr^{-1/7}$	$6.46 \times 10^{-3} Ra^{4/7} Pr^{-6/7}$
IV_l	$\epsilon_{u,bulk}$, $\epsilon_{\theta,bulk}$	$\lambda_u < \lambda_\theta$	$4.43 \times 10^{-4} Ra^{1/2} Pr^{1/2}$	$0.036 Ra^{1/2} Pr^{-1/2}$
IV_u		$\lambda_u > \lambda_\theta$	$0.038 Ra^{1/3}$	$0.16 Ra^{4/9} Pr^{-2/3}$

TABLE 2. The power laws for Nu and Re of the theory presented, including the prefactors which are adopted from four pieces of experimental information in §4. The exact values of the prefactors depend also on how the Reynolds number is defined, see the first paragraph of §4. Regime II_u is in brackets as it turns out that it does not exist for this choice of prefactors.

Boundary between	Pr_{trans}
$I_l - II_l$	$Pr_{trans} = 4.3 \times 10^{-8} Ra_{trans}^{2/3}$
$I_l - III_l$	$Pr_{trans} = 1.0 \times 10^{22} Ra_{trans}^{-2}$
$II_l - IV_l$	$Pr_{trans} = 9.7 \times 10^{10} Ra_{trans}^{-1}$
$III_l - IV_l$	$Pr_{trans} = 9.1 \times 10^{-12} Ra_{trans}^{1}$
$I_u - III_u$	$Pr_{trans} = 5.7 \times 10^{-33} Ra_{trans}^{3}$
$III_u - IV_u$	$Pr_{trans} = 4.8 \times 10^{-8} Ra_{trans}^{2/3}$
$I_l - I_u$	$Pr_\lambda = 2.0 Ra_{trans}^{0}$
$III_l - III_u$	$Pr_\lambda = 5.3 \times 10^{5} Ra_{trans}^{-1/2}$
$IV_l - IV_u$	$Pr_\lambda = 7.3 \times 10^{3} Ra_{trans}^{-1/3}$
I_l-($Re = 50$)	$Pr_{trans} = 6.7 \times 10^{-5} Ra_{trans}^{2/3}$
I_u-($Re = 50$)	$Pr_{trans} = 3.0 \times 10^{-3} Ra_{trans}^{3/5}$
I_l-($Nu = 1$)	$Pr_{trans} = 3.5 \times 10^{4} Ra_{trans}^{-2}$
II_l-($Nu = 1$)	$Pr_{trans} = 1.2 Ra_{trans}^{-1}$
III_u-($Re = 50$)	$Pr_{trans} = 2.9 \times 10^{-5} Ra_{trans}^{2/3}$
II_l-(BL-turbul.)	$Pr_{trans} = 9.3 \times 10^{-12} Ra_{trans}^{2/3}$
IV_l-(BL-turbul.)	$Pr_{trans} = 3.4 \times 10^{-16} Ra_{trans}^{1}$
IV_u-(BL-turbul.)	$Pr_{trans} = 2.3 \times 10^{-11} Ra_{trans}^{2/3}$

TABLE 3. Boundaries between the various regimes I to IV, towards the limiting regimes where $Nu = 1$ (small Pr) and $Re = 50$ (large Pr), and the non-normal-nonlinear onset of shear turbulence (last three lines, see §2.6).

It will turn out that such high shear Reynolds numbers can only be achieved in regimes II and IV; in regimes I and III the large Reynolds numbers necessary for the breakdown of the laminar shear BL are not achieved. With the information from table 2 we obtain the corresponding line in the Ra, Pr parameter space indicating the laminar–turbulence onset range, namely

$$Pr_{turb} \sim Ra_{turb}^{2/3} \tag{2.47}$$

in regimes II_l and IV_u (with different prefactors) and
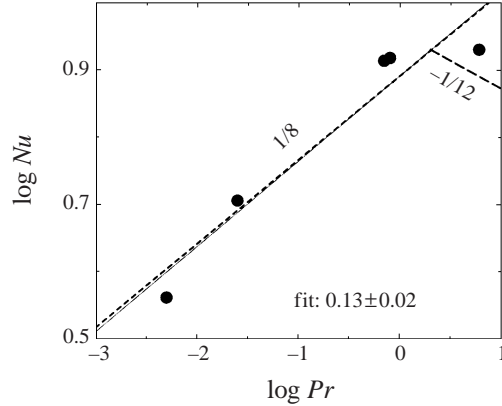
$$Pr_{turb} \sim Ra_{turb}^{1} \tag{2.48}$$

FIGURE 3. *Nu* vs. *Pr* for fixed $Ra = 10^6$. The fit is based on all points. The expected power law $Nu \sim Pr^{1/8}$ in regime I_l is also shown (dashed). For larger $Pr \gtrsim 2$ one enters regime I_u where $Nu \sim Pr^{-1/12}$ (dashed) is expected.

in regime IV_l. The corresponding prefactors will be calculated later, but for clarity we have already included the characteristic lines which mark the onset to turbulence in the BL in the phase diagram figure 2 as dotted line. Above, the RB rolls are still laminar in the boundary layer, below the boundary layer is turbulent.

What power laws for *Re* and *Nu* are to be expected in the regime beyond the turbulence transition of the laminar BL? One might argue that the destruction of the BL laminarity means that both the kinetic and the thermal dissipation rates scale as in the turbulent bulk. This implies that the scaling of *Re* and *Nu* should be the same as in the bulk-dominated regime IV. In the phase diagram we called those regimes II_l', IV_l', and IV_u'.

The same result is obtained by yet another argument: in a turbulent thermal boundary layer (see Landau & Lifshitz 1987; Chavanne *et al.* 1997)

$$\frac{Lu_*}{\kappa} \sim Nu \log\left(\frac{Lu_*}{\kappa}\right). \tag{2.49}$$

With logarithmic precision the typical velocity scale u_* of the fluctuations in the BL is equal to the wind velocity *U* and therefore (2.49) implies $Nu \sim RePr$. On the other hand, still $\epsilon_u \sim \epsilon_{u,bulk}$ or $NuRaPr^{-2} \sim Re^3$. From these two relations one immediately obtains the power laws (2.19) and (2.20), i.e. scaling as in regime IV_l for all three primed regimes II_l', IV_l', and IV_u'.

Still we feel that further study is necessary to obtain reliable insight into the dissipation rate scaling in turbulent boundary layers. This might influence the scaling exponents in the primed regimes II_l' and $IV_{l,u}'$.

3. Comparison with experiment: scaling exponents

3.1. *Nusselt number*

The first type of results of the theory which we would like to compare with experiments is the scaling exponents. First, we focus on the Nusselt number.

For fixed $Ra = 10^6$ *Nu* seems to increase up to $Pr \approx 7$, see figure 3. The fit to the experimental data between $Pr = 0.005$ and $Pr \approx 7$ gives $Nu \sim Pr^{0.13\pm0.02}$ in good agreement with the predicted exponent $\frac{1}{8}$ in regime I_l. We note, however, that the suggestion equation (1.1) by Cioni *et al.* (1997) is also consistent with experiment in the small-*Pr* regime.
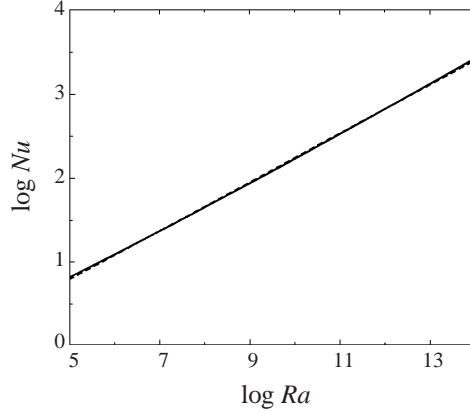
FIGURE 4. *Nu* vs. *Ra* for fixed $Pr = 1$ (characterizing helium) according to the theory presented, i.e. equation (3.1) (solid line). Also shown is the practically indistinguishable result $Nu = 0.22Ra^{0.289}$ of a linear regression of (3.1) (dashed line), which mimics a power law with an exponent close to $\frac{2}{7}$.

The increase with *Pr* seems to cease for *Pr* between 1 and 10. As stated above, other experimental data by Belmonte *et al.* (1994) even suggest a decrease of *Nu* with increasing *Pr* in that regime. This is compatible with and explained by the present theory which gives a (*Ra* independent) transition from the I_l regime with $Nu \sim Pr^{1/8}$ to the regime I_u with $Nu \sim Pr^{-1/12}$, both for fixed *Ra*.

As there is even a controversy in the literature on whether *Nu* for water with $Pr = 6.6$ or *Nu* for helium gas with $Pr = 0.7$ is larger, it is hard to say where exactly the transition from I_l to I_u takes place. According to Cioni *et al.* (1997) it is fair to say that within experimental accuracy $Nu(Pr = 6.6) = Nu(Pr = 0.7)$. We adopt this point of view and use it to calculate the transitional *Pr*, $Pr_{\lambda}^{I_l-I_u}$, to be about 2. This experimental information thus defines the line $\lambda_u = \lambda_\theta$ in the phase space and separates the lower subregime I_l with $\lambda_u < \lambda_\theta$ from the upper subregime I_u with $\lambda_u > \lambda_\theta$.

Next, we compare the predicted scaling exponent γ of *Nu* vs. *Ra*, which in regime *I* is according to our theory the same for the lower and the upper subregimes. For small *Pr* (mercury, sodium) and (relatively) small *Ra* the theoretically obtained value $\gamma = \frac{1}{4}$ for the scaling exponent of *Nu* vs. *Ra* has been measured in several experiments: $\gamma = 0.247$ in Rossby (1969), $\gamma = 0.26 \pm 0.02$ in Cioni *et al.* (1997), and $\gamma = 0.25$ in Horanyi *et al.* (1999).

Also, regime II_l (intermediate *Ra*, low *Pr*) with $\gamma = \frac{1}{5}$ seems to have been observed by Cioni *et al.* (1997).

For larger *Pr* (helium, water) the measured scaling exponent is larger, $\gamma \approx \frac{2}{7}$, see table 1. Here we argue that this results from the superposition of the scaling in regime I, with those in regimes IV_u and III_u. To substantiate this, we plot the expected *Nu* vs. *Ra* dependence for $Pr = 1$,

$$Nu = 0.27Ra^{1/4} + 0.038Ra^{1/3}, \tag{3.1}$$

in figure 4. Here we have made use of the prefactors from table 2, which will be calculated in the next section. Now we fit (3.1) with one power law in as large a range as $10^5 \leqslant Ra \leqslant 10^{14}$. This fit which is nearly indistinguishable from the superposition (3.1) reads

$$Nu = 0.22Ra^{0.289}. \tag{3.2}$$

The power-law exponent is very close to $\frac{2}{7} = 0.286$ and definitely consistent with the experimental data of table 1. Changing the fit range of course changes the exponent of the power law (3.2). For example, for a linear regression in the range $10^6 < Ra < 10^{11}$ which is typical for many experiments one obtains $Nu = 0.24 Ra^{0.285}$, i.e. an exponent which is even closer to $\frac{2}{7}$.

By plotting compensated plots or local slopes $d \log_{10} Nu / d \log_{10} Ra$ as done in figure 5 for (3.1) one may be able to get hints that there is no pure power law. Note that on first sight a compensation with $Ra^{2/7}$ may erroneously even be considered as 'better'.

Chavanne *et al.* (1997) find hints of a transition to a regime with a visibly larger scaling exponent. According to our theory this could be regime III_u or IV_l or IV_l' or, most likely, a mixture of all of them. No clean scaling exponent could hitherto be determined experimentally. One reason is that in that regime both Ra and Pr change. We will discuss the possible nature of this transition below. Also figure 3 of Siggia (1994) suggests such a transition.

We now turn to the large-Pr regime. There are very few data for large $Pr \gg 1$. Recently, Ashkenazi & Steinberg (1999) performed convection experiments with SF_6 close to its critical point. In these experiments both Ra and Pr change considerably at the same time. To what degree the RB convection is still Boussinesq close to the critical point is extensively discussed in Ashkenazi & Steinberg (1999).

Ashkenazi & Steinberg obtain $Nu = 0.22 Ra^{0.3\pm0.03} Pr^{-0.2\pm0.04}$ in $10^9 \leqslant Ra < 10^{14}$ and $1 \leqslant Pr \leqslant 93$. Based on the phase diagram 2 we judge that for these ranges of Ra and Pr we should be in regimes I_u and III_u. From table 2 we see that the Ra exponent of Nu is $\frac{1}{4}$ and $\frac{3}{7}$, respectively. The measured exponent of 0.3 ± 0.03 in between is consistent with this. The Pr exponent of Nu is expected to be in between $-\frac{1}{12}$ and $-\frac{1}{7}$, slightly smaller (modulus-wise) than the value of -0.2 ± 0.04 reported in Ashkenazi & Steinberg (1999).

The results of this subsection clearly demonstrate the importance of superimposing the power laws of adjacent phase-space regimes. This can really mimic different scaling behaviour, as demonstrated in figures 4 and 6. This characteristic feature holds because the power-law exponents of neighbouring regimes are rather similar. They will commonly appear if data in a crossover range are examined. We emphasize that these crossover ranges appear to be rather extended, reaching well into the corresponding regimes, due to the small differences of the scaling exponents.

Therefore, rather than writing pure power laws, one should allow for superpositions. Table 2 suggests

$$Nu \sim Ra^{1/4} Pr^{1/8} \left(1 + \begin{cases} c_{III_u} & Ra^{5/28} Pr^{-15/56} + \cdots \\ c_{IV_u} & Ra^{1/12} Pr^{-1/8} + \cdots \\ c_{IV_l} & Ra^{1/4} Pr^{3/8} + \cdots \\ c_{II_l} & Ra^{-1/20} Pr^{3/40} + \cdots \end{cases} \right) \tag{3.3}$$

and

$$Re \sim Ra^{1/2} Pr^{-3/4} \left(1 + \begin{cases} c'_{III_u} & Ra^{1/14} Pr^{-3/28} + \cdots \\ c'_{IV_u} & Ra^{-1/18} Pr^{1/12} + \cdots \\ c'_{IV_l} & Pr^{1/4} + \cdots \\ c'_{II_l} & Ra^{-1/10} Pr^{3/20} + \cdots \end{cases} \right), \tag{3.4}$$
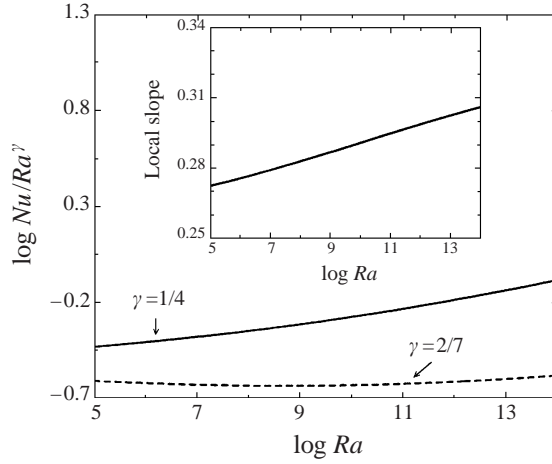
FIGURE 5. *Nu* from (3.1), compensated by two different power laws: $Ra^{1/4}$ (solid, as suggested by the present theory for the low-*Ra* regime) and $Ra^{2/7}$ (dashed). The second is hardly distinguishable from a straight line, i.e. pure $\frac{2}{7}$ scaling. The inset shows the local slope following from (3.1).
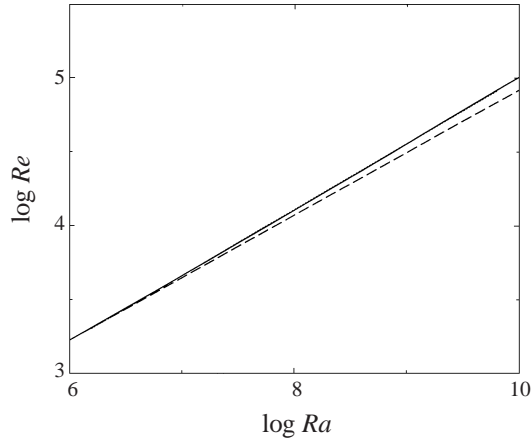

FIGURE 6. *Re* vs. *Ra* for mercury, $Pr = 0.025$. The solid line shows the theoretical superposition $0.59Ra^{1/2} + 4.30Ra^{2/5}$ which is very well fitted by a straight line $Re = 3.5Ra^{0.446}$ (dotted, practically indistinguishable from the solid line; the fit interval is $Ra = 10^6$ to $Ra = 4 \times 10^9$ as in the experiment). The dashed line presents Cioni *et al.*'s fit through their data $Re \propto Ra^{0.424}$. The prefactors cannot be compared because of the different definitions of the Reynolds number in Chavanne *et al.* (1997) and Cioni *et al.* (1997), see §4, first paragraph.

respectively. Here, we have separated the exponents of regime I_l. Which of these corrections and how many are to be taken depends on *Pr* and on the aspect ratio. Locally, i.e. for a limited *Ra* range, the suggested *Nu* vs. *Ra* power-law exponents $\gamma = \frac{2}{7}$ (Castaing *et al.* 1989; Shraiman & Siggia 1990) (cf. figure 2 of Chavanne *et al.* 1997 or figure 3 of Siggia 1994), or $\gamma = \frac{5}{19}$ suggested by Yakhot (1992) can still be considered as an appropriate representation of the experimental data. Globally, for larger *Ra* intervals, however, we claim that (3.3) is a better description.

In previous publications *Nu*, compensated by the expected scaling $Ra^{2/7}$, was plotted against *Ra* in a log-log plot, see figure 2 of Chavanne *et al.* (1997). From that plot one realizes that the $\frac{2}{7}$-scaling is slightly too steep between $Ra = 10^6$ and
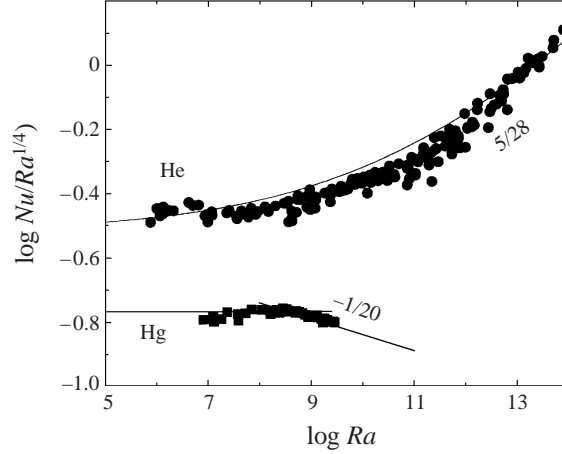
FIGURE 7. Compensated *Nu* vs. *Ra* data for *Pr* from about 1 to about 20 (helium, upper, data taken from Chavanne *et al.* 1997; the higher *Ra* experiments also have higher *Pr*) and *Pr* = 0.025 (mercury, lower, taken from Cioni *et al.* 1997). Also shown are the calculated exponents in the large-*Ra* regimes. We also drew the theoretical curve $Nu = 0.33 Ra^{1/4} Pr^{-1/12} + 3.43 \times 10^{-3} Ra^{3/7} Pr^{-1/7}$ with fixed *Pr* = 3 to demonstrate that it roughly describes the data. If the expected *Pr* dependence is considered, the agreement becomes even better.

$Ra = 10^8$ and not steep enough beyond the crossover at $Ra = 10^{11}$. The analogously compensated plot with the expected scaling (2.31) is shown in figure 7. Now (for $Pr \approx 1$) one obtains a horizontal line up to $Ra \approx 10^9$, showing that (2.31) nicely agrees with the data. However, beyond $Ra \approx 10^9$ one observes deviations. We suggest that these corrections originate from the different scaling in the neighbouring regime III_u. The reason that it is regime III_u (and not regime IV_u) is that in the Chavanne *et al.* experiments the large-*Ra* measurements also have large *Pr*; the trajectory in control parameter space *Ra*, *Pr* is not a straight line. At $Ra = 10^{10}$ one typically has $Pr \approx 1$, but at $Ra = 10^{14}$ Chavannve *et al.* typically have $Pr \approx 10$–20. The power law exponent $\frac{5}{28}$, following from table 2, is consistent with the experimental data for large *Ra*, see figure 7.

For the mercury data of Cioni *et al.* (1997) we do not have such a complication as $Pr = 0.025$ is roughly constant for all chosen *Ra*. As plotted in figure 7, lower curve, we observe a straight line up to about 2×10^8 and then a decay, signalling contributions from regime II_l. The power law exponent $-\frac{1}{20}$ of the correction term in (3.3) is consistent with the data shown in figure 7.

A more stringent way to test the superpositions of type (3.3) is to make a linear plot $Nu/(Ra^{1/4} Pr^{1/8})$ vs. $Ra^{5/28} Pr^{-15/56}$ or vs. $Ra^{1/12} Pr^{-1/8}$ or vs. $Ra^{1/4} Pr^{3/8}$, etc., depending on from which neighbouring regime the corrections originate. This is done in figure 8, assuming, as argued above, that the most relevant corrections originate from regime III_u. If the theory is correct, the data points must fall on a straight line. Indeed, they do so with satisfying precision.

Note that this kind of linear plot is very sensitive to what combinations of *Ra* and *Pr* are chosen as x- and y-axes. For example, plotting $Nu/(Ra^{1/4} Pr^{1/8})$ vs. $Ra^{1/4} Pr^{3/8}$ (the subleading correction characterizing regime IV_l) does not lead to a straight line at all, see the inset of figure 8. Clearly the variable $Ra^{5/28} Pr^{-15/56}$ on the abscissa is superior, adding confirmation that the large-*Ra* experiments by Chavanne *et al.* (1997) represent the physics of regime III_u.
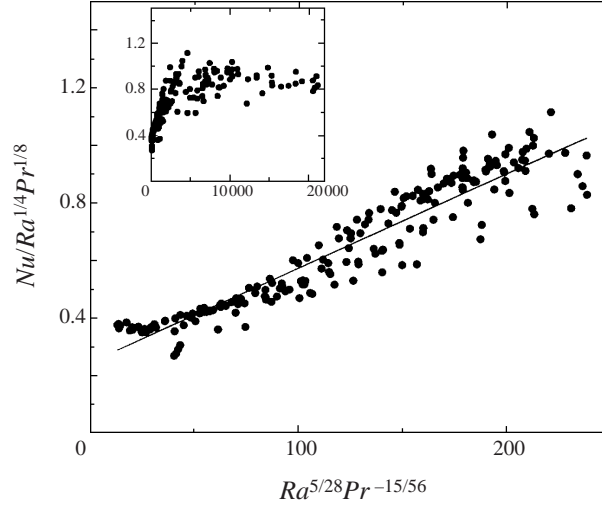
FIGURE 8. Same data as in figure 7, but now in a linear plot $Nu/(Ra^{1/4}Pr^{1/8})$ vs. $Ra^{5/28}Pr^{-15/56}$, revealing the quality of the superposition (3.3), high-Pr, regime III_u. The linear fit (straight line) gives $Nu/(Ra^{1/4}Pr^{1/8}) = 0.24 + 3.3 \times 10^{-3}Ra^{5/28}Pr^{-15/56}$. The data points are taken from Chavanne *et al.* (1997), with kind permission by the authors. Only data points with $Ra > 10^6$ are considered. Note that in this plot Pr varies as much as $0.6 < Pr < 100$. The inset shows $Nu/(Ra^{1/4}Pr^{1/8})$ vs. $Ra^{1/4}Pr^{3/8}$; this variable had to be used if regime IV_l contributes the most relevant correction. The data do not fall on a straight line. A similar failure results with the regime IV_u-compensated variable $Ra^{1/12}Pr^{-1/8}$.

3.2. *Reynolds number*

We now consider the experimental values for the scaling exponents α of the Reynolds number vs. the Rayleigh number. For $Pr \approx 7$ (water) Xin *et al.* (1996) find $\alpha = 0.50 \pm 0.01$ and Qiu & Xia (1998) find $\alpha = 0.50 \pm 0.02$. Both experiments were done in the Ra interval between 2×10^8 and 2×10^{10}, i.e. in regime I_u, where exactly this power law exponent $\alpha = \frac{1}{2}$ is expected. For $Pr \approx 1$ both Castaing *et al.* (1989) and Chavanne *et al.* (1997) find $\alpha = 0.49$ for all Ra which suggests that possibly the regimes I_l and IV_l are seen where this value is predicted, and (according §3.1) also regime III_u, where the exponent is only slightly higher ($\frac{4}{7}$). For $Pr = 0.025$ (mercury) Cioni *et al.* 1997 find $\alpha = 0.424$ from a fit to all available Ra. This value is in between the derived values $\alpha = \frac{1}{2}$ in regime I_l and $\alpha = \frac{2}{5}$ in regime II_l.

We compare this experimental finding $Re \propto Ra^{0.424}$ (based on a fit to the data in the range up to $Ra = 4 \times 10^9$ by Cioni *et al.* 1997) with the I_l–II_l superposition according to table 2

$$Re = 0.59Ra^{1/2} + 4.30Ra^{2/5}, \tag{3.5}$$

cf. figure 6. In this relatively short Ra interval the theoretical superposition (3.5) is again hardly distinguishable from its straight line fit

$$Re = 3.5Ra^{0.446} \tag{3.6}$$

whose exponent agrees reasonably well with the measured one.†

Moreover, the theoretically obtained Pr dependence of Re also agrees very nicely with available experimental information: Chavanne *et al.* (1997) did experiments

---

† The absolute values of the Reynolds numbers cannot be compared here, as the Reynolds number definitions in Cioni *et al.* 1997 and Chavanne *et al.* (1997) cannot be translated into each other, see the first paragraph in §4.
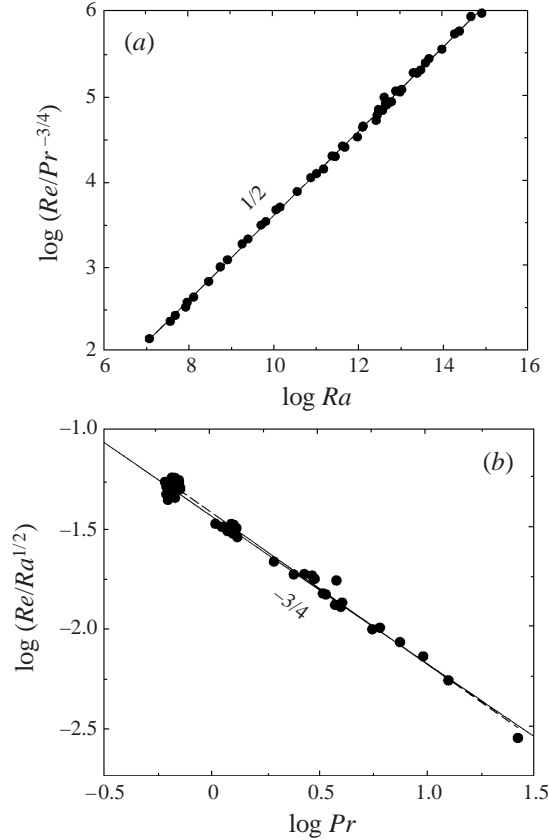
FIGURE 9. Data for the Reynolds number as a function of Ra and Pr from Chavanne *et al.* (1997), with very kind permission of the authors. (*a*) $Re/Pr^{-3/4}$ vs. Ra. The expected slope (in regimes $I_{e,u}$ and IV_e) is $\frac{1}{2}$, the linear regression fit (solid line) gives 0.492 ± 0.002. (*b*) $Re/Ra^{1/2}$ vs. Pr. The expected slope is $-\frac{3}{4}$ for $Pr \leqslant 2$ (regime I_l) and $-\frac{5}{6}$ for $Pr \geqslant 2$ (regime I_u). The linear regression fit (dashed line) gives -0.77 ± 0.01. The agreement of the prefactor is also excellent. According to theory, following table 2 it is $\log_{10}(Re/Ra^{1/2}) = -1.432 - (\frac{3}{4})\log_{10} Pr$ (solid line, hardly distinguishable from the dashed one); the fit value for the prefactor from linear regression is -1.413 ± 0.005. According to §3.1, the large-Pr data, when Ra is also large, may be in regime III_u and the slope should be slightly steeper $(-6/7)$.

with (slightly) varying Pr. They then plotted $RePr^{0.72}$ vs. Ra and obtained the law $RePr^{0.72} = 0.0374 Ra^{1/2}$. The exponent 0.72 of the Prandtl number was determined by minimizing the scattering of points around a straight line in the log-log plot. It agrees very well with the calculated Pr scaling exponent $\frac{3}{4}$ in (2.32) (regime I_l). A possible reason for the slight difference between theory and data fit is that part of the experimentally realized Ra and Pr already belong to regimes III_u and IV_u, where according to (2.20) and (2.22) the expected Pr scaling exponent is $\frac{6}{7}$ and $\frac{2}{3}$, respectively. However, the deviation is clearly within the experimental uncertainty. In figure 9 we replot the experimental Reynolds number data of Chavanne *et al.* (1997). In figure 9(*a*) we show $Re/Pr^{-3/4}$ vs. Ra. The fit gives a Ra exponent 0.492 ± 0.002 in very good agreement with the theory's exponent $\frac{1}{2}$ of regimes I and IV_l; that of regime III_u is slightly larger (4/7). In figure 9(*b*) we display $Re/Ra^{1/2}$ vs. Pr. The data fit results in a Pr exponent -0.77 ± 0.01, also in excellent agreement with the theoretical expectation which is $-\frac{3}{4}$ in I_l and $-\frac{5}{6}$ in I_u.

The large Ra values in both figures 9(*a,b*) will turn out to belong to the regimes III_u (see also §3.1 on the Nusselt number) and IV_u, where the Pr-scaling is similar. The available range is too small to perform a more detailed comparison.

The only large-Pr data available are again those by Ashkenazi & Steinberg (1999). They obtain $Re = 2.6Ra^{0.43\pm0.02}Pr^{-0.75\pm0.02}$ in $10^{12} \leqslant Ra < 3\times10^{14}$ and $27 \leqslant Pr \leqslant 190$. The expected Ra exponent of Re is between $\frac{1}{2}$ and $\frac{4}{7}$, distinctly larger than the measured one of 0.43 ± 0.02. Similarly, the theoretically expected Pr exponent of Re is between $-\frac{5}{6}$ and $-\frac{6}{7}$, also larger than the measured exponent -0.75 ± 0.02. We have no explanation.

4. Prefactors

4.1. *Experimental input to determine the prefactors*

To obtain the values of the prefactors in the power laws within the presented scaling theory, we need further input from experiment. But what data to choose? As pointed out in the introduction, a huge variety of data is around, often disagreeing with each other even in the scaling exponents, not to speak of prefactors. Those often vary by as much as 50% from experiment to experiment, even for cells with the same aspect ratio. Another reason which makes the adoption of one experiment and the comparison to others difficult is that different definitions are used for the Reynolds numbers. For example, Cioni *et al.* (1997) define the Reynolds number as $Re = 4L^2 f_p/\nu$, where f_p is a distinguished frequency at the small-frequency end of the temperature spectrum. Chavanne *et al.* (1997) define $Re = \omega_0 dL/\nu$, where ω_0 is a typical frequency in the cross-correlation spectrum of two temperature signals, measured at a vertical distance of $d = 2.3$ mm and 2 cm off the axis of the cell.

In spite of these difficulties, we decided to calculate the prefactors of the suggested scaling laws by employing the following choice for the input information as a reasonable, realistic example. Our reasons are first to be able to draw a phase diagram with more or less realistic values and second to stress the importance of the prefactors. But we caution the reader that our input choice is somewhat arbitrary; other possibilities can equally well be rationalized, sometimes shifting the various regime boundaries considerably.

Above, as an input from experiment, we had chosen $Pr_\lambda = 2$ as the Prandtl number for which Nu is maximal (for fixed $Ra = 10^6$, cf. figure 3). In addition, we will use the following experimental information:

(*a*) the observed transition Rayleigh number for the transition from regime I_l to regime III_l, $Ra_{trans} = 10^{11}$ at $Pr = 1$ by Chavanne *et al.* (1997);

(*b*) the observed transition Rayleigh number for the transition from regime I_l to regime II_l, $Ra_{trans} = 4.5 \times 10^8$ at $Pr = 0.025$ by Cioni *et al.* (1997);

(*c*) the experimental values, taken from Chavanne *et al.* (1997), for the Reynolds and the Nusselt number at the middle point (Ra_M, Pr_M) in the phase diagram figure 2;

(*d*) the prefactor 0.0372 of the scaling law $Re = 0.0372Ra^{1/2}Pr^{-3/4}$ measured in regime I_l, taken from Chavanne *et al.* (1997).

Information (*a*) specifies the prefactor of the right-hand side of (2.40) (which we call $c_{I_l-III_l}$) to be $c_{I_l-III_l} = Pr_{trans}^{I_l-III_l}/Ra_{trans}^{-2} = 1.0 \times 10^{22}$. Information (*b*) gives the prefactor of the right-hand side of (2.39) (which we call $c_{I_l-II_l}$) to be $c_{I_l-II_l} = Pr_{trans}^{I_l-II_l}/Ra_{trans}^{2/3} = 4.3 \times 10^{-8}$. The two curves (2.39) and (2.40) cross at

$$(Ra_M, Pr_M) = (1.03 \times 10^{11}, 0.94). \tag{4.1}$$

This middle point (Ra_M, Pr_M) is defined by the conditions $\epsilon_{u,BL} = \epsilon_{u,bulk} = \epsilon_u/2$ and

$\epsilon_{\theta,BL} = \epsilon_{\theta,bulk} = \epsilon_\theta/2$. Equation (4.1) specifies the prefactors of the right-hand sides of (2.41) and (2.42) to be $c_{III_l-IV_l} = 9.1 \times 10^{-12}$ and $c_{II_l-IV_l} = 9.7 \times 10^{10}$, respectively. We see that $Pr_\lambda^{I_l-I_u} = 2 > Pr_M = 0.94$ so that there is a regime III_l, but no regime II_u, as already anticipated. The line $Pr_\lambda^{I_l-I_u} = 2$ hits the boundary between I and III at

$$(Ra_{M'}, Pr_{M'}) = (7.1 \times 10^{10}, 2.0), \qquad (4.2)$$

which fixes the prefactors of (2.43) and (2.37) to be 5.7×10^{-33} and 5.3×10^5, respectively. Correspondingly, one obtains the prefactors of (2.44) and (2.38) to be 4.8×10^{-8} and 7.3×10^3, respectively. These are the data on which the phase diagram figure 2 is based; they are summarized in table 3.

Apart from III_l all regimes turned out to extend at least one decade of both in Ra and in Pr and should therefore in principle be visible. However, we should always expect one or more subleading corrections. Regime III_l will clearly not be detectable.

We again stress how dependent this phase diagram drawn in figure 2 is on the choice of experimental information. For example if we had adopted the point of view by Glazier *et al.* (1999) that there is no transition towards a steeper Ra dependence of Nu at least up to $Ra = 8 \times 10^{10}$, regimes II and IV would have shifted further to the right or would even not exist at all. But as shown in figure 4, apparent smooth scaling behaviour does not allow a transition to be excluded.

Making use now of the experimental information (*c*) and (*d*) we can calculate the prefactors in the power laws for Nu and Re. From figures 2 and 3 of Chavanne *et al.* (1997) we can extract the Reynolds and Nusselt numbers at the middle point (Ra_M, Pr_M) of the phase diagram which touches all four regimes, namely

$$Re_M = 1.20 \times 10^4, \qquad Nu_M = 2.78 \times 10^2, \qquad (4.3)$$

which is information (*c*) above. The definition of the middle point (Ra_M, Pr_M), i.e. the conditions $\epsilon_{u,BL} = \epsilon_{u,bulk} = \epsilon_u/2$ and $\epsilon_{\theta,BL} = \epsilon_{\theta,bulk} = \epsilon_\theta/2$, allows us to calculate the prefactors $c_{\epsilon_u,bulk}$, $c_{\epsilon_\theta,bulk}$, and $c_{\epsilon_u,BL}$ on the right-hand sides of (2.11), (2.12), and (2.14), respectively. One obtains

$$c_{\epsilon_u,bulk} = \frac{Nu_M Ra_M}{2 Pr_M^2 Re_M^3} = 9.38, \qquad (4.4)$$

$$c_{\epsilon_\theta,bulk} = \frac{Nu_M}{2 Pr_M Re_M} = 0.0123, \qquad (4.5)$$

$$c_{\epsilon_u,BL} = \frac{Nu_M Ra_M}{2 Pr_M^2 Re_M^{5/2}} = 1028. \qquad (4.6)$$

Finally, the prefactor c_{Nu} on the right-hand side of relation (2.17) is adopted from Chavanne *et al.*'s (1997) experimentally determined prefactor (see figure 3 of that paper) in the relation (2.32), i.e. $Re = 0.0372 Ra^{1/2} Pr^{-3/4}$ valid throughout regime I_l (information (*d*) above). In that regime $\epsilon_{u,BL} = \epsilon_u$; with (2.5), (2.14), and (4.6) we get

$$c_{Nu} = (3.72 \times 10^{-2})^2 c_{\epsilon_u,BL} = 1.42. \qquad (4.7)$$

The prefactors referring to the upper half of the phase diagram are calculated from the matching conditions for Re and Nu on the $\lambda_u = \lambda_\theta$ line. With (4.4)–(4.7) and the matching conditions now all prefactors of the power laws in the four different regimes are determined. We have summarized all these power laws in table 2.

Note that from the condition $\lambda_u = \lambda_\theta$ for $Pr = 2$ the prefactor of (2.8) is also obtained. It is 0.25, i.e. $\lambda_u = 0.25 L Re^{-1/2}$. Also the prefactors to the $Nu = 1$ and the $Re \leqslant 50$ borders of validity and the crossover lines to turbulence of the laminar BL flow automatically follow, and are included in table 2.

4.2. *Comparison of the evaluated prefactors to experiment*

We now would like to compare the absolute agreement of the power laws summarized in table 2, whose prefactors result from an adoption to the above four pieces of experimental information, with further experimental data. We first focus on the Chavanne *et al.*'s (1997) RB measurements in helium gas. From the previous section we know that in these experiments due to the large Pr at large Ra it is mainly regime III_u which causes additional contributions to regime I_l. Therefore, we have plotted the superposition $Nu = 0.33 Ra^{1/4} Pr^{-1/12} + 3.43 \times 10^{-3} Ra^{3/7} Pr^{-1/7}$ with $Pr = 3$ on figure 7. We again stress that in the experiments Pr is not constant at all. Nevertheless, the data are satisfactorily described. Note that the solid curve in figure 7 is no fit!

A much better way to check whether the prefactors of the theory obtained agree with the measured ones is to do a linear regression of the straight line as in figure 8. Such a straight line fit gives $Nu/(Ra^{1/4} Pr^{1/8}) = 0.24 + 3.3 \times 10^{-3} Ra^{5/28} Pr^{-15/56}$. The prefactors found are in good agreement with the expectation $Nu/(Ra^{1/4} Pr^{1/8}) = 0.27 + 3.43 \times 10^{-3} Ra^{5/28} Pr^{-15/56}$ from table 2.

We also compare the theoretical prefactors of the Reynolds number scaling in regime I_l with experiment. As the theoretical prefactors have been adopted from the experimental $Re/Pr^{-3/4}$ vs. Ra power law, it only makes sense to check the prefactors in $Re/Ra^{1/2}$ vs. Pr. From table 2 in I_l the expected slope is $-\frac{3}{4}$ and the expected prefactor 0.037; in I_u the expected slope is $-\frac{5}{6}$ and the expected prefactor is 0.039. Linear regression of the whole regime $I_l + I_u$ gives a slope of -0.77 ± 0.01 and a prefactor of $10^{-1.413 \pm 0.005} = 0.0386$, cf. figure 9. It is of course more correct to fit the two regimes separately: linear regression of the regime I_l gives a slope of -0.81 ± 0.04 and a prefactor of 0.038; linear regression of the regime I_u gives a slope of -0.81 ± 0.03 and a prefactor of 0.042, all values being consistent with the expectation.

Next, we compare the experimental Nu vs. Ra scaling for mercury with $Pr = 0.025$ with theory. The measured relations $Nu = (0.140 \pm 0.005) Ra^{0.26 \pm 0.02}$ by Cioni *et al.* (1997), $Nu = 0.147 Ra^{0.257}$ by Rossby (1996), and $Nu = 0.155 Ra^{0.27}$ by Takeshita *et al.* (1996) are all in reasonable agreement with the regime I_l expectation $Nu = 0.17 Ra^{1/4}$ from table 2. The same holds for a comparison in regime II_l: the reported experimental fit is $Nu = 0.44 \pm 0.015 Ra^{0.20 \pm 0.02}$ (see Cioni *et al.* 1997), theory gives $Nu = 0.46 Ra^{1/5}$, again, remarkable agreement of both the power-law exponent and the prefactor. Remember that the only experimental input from this experiment into the theory is $Ra_{trans}^{I_l - II_l} = 4.5 \times 10^8$.

Let us also check the prefactors of Nu as a function of Pr for fixed $Ra = 10^6$. A power-law fit to all available experimental data points taken from Cioni *et al.* (1997) and Horanyi *et al.* (1999) included in figure 3 gives $Nu = (7.8 \pm 0.5) Pr^{0.13 \pm 0.02}$ which is in agreement with the theoretical expectation $Nu = 0.27 Ra^{1/4} Pr^{1/8} = 8.5 Pr^{1/8}$ in regime I_l. Leaving out the data points for water ($Pr = 7$) which already belongs to regime I_u gives a slightly larger power-law exponent and a slightly larger prefactor, $Nu = 8.7 Pr^{0.16}$. But both exponent and prefactor are still consistent with the theoretical expectation.
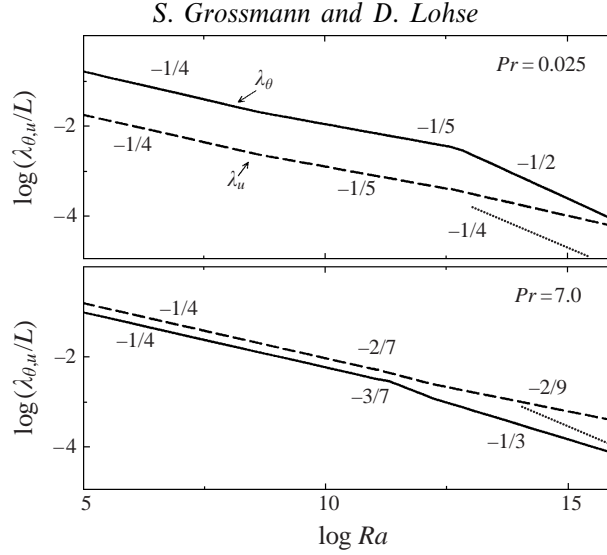
FIGURE 10. Widths of the boundary layers $\lambda_\theta = 0.5LNu^{-1}$ (solid) and $\lambda_u = 0.25LRe^{-1/2}$ (dashed) for mercury ($Pr = 0.025$, upper) and water ($Pr = 7.0$, lower). The dotted lines show the thicknesses y_0 of the viscous sublayers of a turbulent boundary layer, calculated according to (4.10). Such a width is expected beyond the non-normal-nonlinear transition to turbulence of the laminar shear BL (cf. §2.6).

4.3. *Widths of the boundary layers*

As stated above, the present theory also gives the absolute widths of the thermal and the laminar viscous boundary layers,

$$\lambda_\theta = 0.5LNu^{-1}, \tag{4.8}$$

$$\lambda_u = 0.25LRe^{-1/2}. \tag{4.9}$$

The results for the widths of the BLs for $Pr = 0.025$ (mercury) and $Pr = 7.0$ (water) are shown in figure 10. In both cases there are three regimes involved, namely I_l, II_l, and IV_l for $Pr = 0.025$ and I_u, III_u, and IV_u for $Pr = 7.0$. As expected, for the larger Pr the thermal boundary layer is always nested in the viscous one which agrees with the experimental observations by Belmonte *et al.* (1994). For the lower Pr it is the other way round.

If the laminar BL becomes turbulent, the Blasius estimate $\lambda_u \sim LRe^{-1/2}$ for its width must be replaced by the thickness of the turbulent BL. To give an idea of this length scale, we calculate the width y_0 of the viscous sublayer of the turbulent BL within the Prandtl theory (see Landau & Lifshitz 1987), applied to Couette flow. In the large-Re limit (see again Landau & Lifshitz 1987 and our unpublished material on the prefactor)

$$\frac{y_0}{L} = 1.38 \frac{\log(k^2 Re)}{k^2 Re}. \tag{4.10}$$

Here, $k = 0.4$ is the experimentally known von Kármán constant. We have included y_0/L in figure 10 for the relevant large Ra. The turbulent viscous sublayer is thiner than the laminar BL. One also notes that for the larger Prandtl number $Pr = 7$ (water) the assumption by Shraiman & Siggia (1990) of the thermal boundary layer being nested in the turbulent one is just fulfilled. For lower Pr this is not the case any more.

Many experiments justify the identification of the thermal BL width with the

inverse Nusselt number, $\lambda_\theta = 0.5 L N u^{-1}$. For a detailed discussion we refer to the review articles or to Belmonte *et al.* (1994) or to the more recent work by Lui & Xia (1998).

The situation is more complicated for the width of the kinetic BL λ_u. Its measurement is experimentally difficult. Moreover, experimental results on λ_u seem to exist only for regime *I*.

Belmonte *et al.* (1994) tried to measure λ_u in an indirect way, namely through the detection of a spectral cutoff frequency in gas convection which in water convection (at one Ra) is found to have a similar dependence on the height z in the RB cell as the velocity profile $U(z)$. For $Pr \approx 1$ they found $\lambda_u \approx$ const in the range $2 \times 10^7 \leqslant Ra \leqslant 2 \times 10^9$ and $\lambda_u \sim L Ra^{-0.44 \pm 0.09}$ in $2 \times 10^9 \leqslant Ra \leqslant 10^{11}$. We have no idea about the origin of the measured scaling exponents.

More recently, Xin *et al.* (1996), Xin & Xia (1997), and Qiu & Xia (1998) measured the thickness of the kinetic BL in a water cell in a more direct way. They define λ_u as the distance from the wall at which the extrapolation of the linear part of the velocity profile $U(z)$ equals the maximum velocity $U = \max_z U(z)$, the velocity of the large-scale wind. In the interval $2 \times 10^8 \leqslant Ra \leqslant 10^{10}$ they find $\lambda_u \sim L Ra^{-0.16 \pm 0.02}$ for the thickness of the top and bottom kinetic BL (see Xin *et al.* 1996; Xin & Xia 1997) and $\lambda_u \sim L Ra^{-0.26 \pm 0.03}$ for the thickness of the kinetic BLs at the sidewalls (see Qui & Xia 1998). The first exponent (for the top and the bottom plates) is different from the value from this theory $\lambda_u \sim L Ra^{-1/4}$. The power law for the thickness of the kinetic BLs at the sidewalls, however, is in good agreement with the expectation $\lambda_u \sim L Ra^{-1/4}$.

We can only speculate on the origin of this discrepancy of the scaling exponent of the width of the bottom and top walls. Perhaps, if λ_u is defined as the distance of the velocity maximum to the wall, the Ra-scaling would be different. The different scaling exponents at the top/bottom walls and at the sidewalls may also reflect the role of the plumes at the top/bottom wall which are not explicitly embodied in the present theory.

In any case, the experimentally found very weak dependence of λ_u on Ra supports the assumed laminar nature of the kinetic BL, apart from possible intermittent bursts through plumes. However, if the width of the BL were identified with the width y_0 of the viscous sublayer of a turbulent BL, one would expect a stronger dependence on Re, namely $y_0 \sim L \log(k^2 Re)/(k^2 Re)$ (see Landau & Lifshitz 1987), i.e. when neglecting logarithmic corrections, one would have $y_0 \sim L/Re \sim L Ra^{-1/2}$.

4.4. *Experimental evidence for the turbulence onset in the BL*

According to the presented theory with the chosen prefactors the breakdown of laminarity in the shear BL happens at $Ra_{turb} \approx 10^{16}$ for $Pr = 1$ and $Ra_{turb} \approx 10^{14}$ for $Pr = 0.025$. These values are calculated from table 3. Hitherto, there have been no experiments on these regimes.

However, one may want to argue that the transition to a turbulent shear BL may already occur earlier, be it because of a different aspect ratio, or, in view of more recent work by Eckhardt & Mersmann (1999) and Schmiegel & Eckhardt (1999), because the critical Reynolds number (which we had assumed to be 420, cf. (2.46)) is smaller, or because of a different choice of the experimental input information from which the prefactors of the theory are adopted. For example, if one assumes a laminar shear layer with width $\lambda_u = 1.72 L/\sqrt{Re}$ as suggested by Landau & Lifshitz 1987, section 39), for the (related) case of a flat-plate shear flow, the transition to turbulence in the shear BL has already occured at $Ra_{turb} = 10^{13}$ (for $Pr = 4$). We note

that this is just at about that Ra where Procaccia *et al.* (1991) measured a marked transition in the (thermal) dissipative spectral power by a probe placed in the BL. This transition was towards a weaker increase with Ra.

In the context of this section we also interpret the above-mentioned recent experiment by Ciliberto & Laroche (1999) in which the boundary layers are disturbed by constructing a rough bottom plate with a mean roughness comparable to the thermal boundary layer thickness. The experiments are performed in water. According to the theory of this paper one would expect larger bulk contributions to both the thermal and the kinetic dissipation and therefore an earlier onset of regimes III_u' and IV_u'. Indeed, experimentally the increase of Nu with Ra is found to be much steeper. For the experiment described by Ciliberto & Laroche (1999) the data can be fitted to power laws $Nu \sim Ra^{0.35}$ or $Nu \sim Ra^{0.45}$, depending on the features of the rough bottom and upper plate.

5. Summary and conclusions

We summarize the central ingredients of the theory presented in this paper. The scaling laws for the Nusselt number and the Reynolds number are based on the decomposition of the global thermal and kinetic energy dissipation rates into their BL and bulk contributions. These in turn are estimated from the dynamical equations, taking the wind U as the relevant velocity in the heat conduction cell. The resulting estimates are inserted into the rigorous relations (2.5) and (2.6) for the global kinetic and thermal energy dissipation, respectively. Four regimes arise, depending on whether the bulk or the BL contributions dominate the two global dissipations. Each of the four regimes in principle divides into two subregimes, depending on whether the thermal BL (of width λ_θ) or the kinetic BL (of width λ_u) is larger.

In addition to these main regimes there is a range for very large Pr in which the wind Reynolds number is $\leqslant 50$; here the whole flow is viscosity dominated, and the theory loses its applicability. There also is the range of very small Pr in which Nu goes down to $Nu = 1$, and again the theory no longer holds. Finally, for large Ra the laminar kinetic BL becomes turbulent. Beyond turbulence onset we feel the flow is bulk dominated.

All scaling exponents follow from this theory. If one in addition introduces only four pieces of experimental information, all the prefactors can also be determined. Therefore the theory has predictive power not only for the power-law exponents but also for the prefactors. These, however, depend on the chosen experimental information input. To confirm the prefactors more input information for various aspect ratios is necessary.

The phase diagram of the theory, the main result of this work, is shown in figure 2. The power laws with the prefactors based on the chosen experimental information are summarized in table 2, the power laws of the boundaries between the different regimes in table 3.

A detailed comparison of the theoretical power-law exponents and the prefactors with the experimental data gives reasonable and encouraging agreement. We emphasize that to accurately account for the dependences of Nu and Re on Ra and Pr single power laws are often not sufficient, as additive corrections from neighbouring regimes can be considerable. This can be viewed as one of the main insights obtained in this paper. A particularly striking example is that $Nu = 0.27 Ra^{1/4} + 0.038 Ra^{1/3}$ mimics a $\frac{2}{7}$ power-law scaling over at least nine order of magnitude in Ra, see figure 4.

The theory also offers a possible explanation why a transition to a steeper increase

of Nu vs. Ra is seen in the data by Chavanne *et al.* (1997), but not in the Chicago group data (Castaing *et al.* 1989; Wu 1991; Procaccia *et al.* 1991). It may be that in the large-Ra Chicago experiments Pr was smaller than in the measurements by Chavanne *et al.* (1997). Then for the Chicago data one should expect a transition towards regime IV_u† where the Ra scaling exponent is $\frac{1}{3}$ and thus, as demonstrated, superposed on the leading $\frac{1}{4}$ exponent, is indistinguishable from a $\frac{2}{7}$ scaling. In the Chavanne *et al.* (1997) experiments, on the other hand, one has the transition to the large-Pr regime III_u where the Ra scaling exponent is $\frac{3}{7}$ which is much more distinguishable from $\frac{1}{4}$. Whether this explanation is true remains to be seen.

What we consider as most serious discrepancy between the theory presented and the available data is the measured weak Ra dependence of the width of the kinetic BL at the top and bottom walls, $\lambda_u \sim LRa^{-0.16\pm0.02}$ (Xin *et al.* 1996; Xin & Xia 1997), whereas this theory predicts $\lambda_u \sim LRa^{-1/4}$ (which coincides with the measured result at the sidewalls (Qiu & Xia 1998)). Perhaps by explicitly embodying plumes and fluctuations in the kinetic BL this discrepancy can be resolved. Note again that for Ra at least up to order of 10^{11} the kinetic BL layer cannot be turbulent. If so, this would even imply $\lambda_u \sim LRa^{-1/2}$.

Finally, we want to stress and discuss one of the basic assumptions of the theory, namely, that a large-scale 'wind of turbulence' exists, defining the Reynolds number $Re = UL/v$, creating a shear BL and stirring the turbulence in the bulk. Clearly, this assumptions breaks down in the shaded area in figure 2 beyond the line $Re = 50$ where the flow is viscosity dominated. But even below this line we do not exclude that the convection rolls break down and that the heat is exclusively transported by the fluctuations. For example for a water cell ($Pr \approx 7$) Tanaka & Miyata (1980) do not note the wind of turbulence, in contrast to Zocchi *et al.* (1990), who do observe it in their experiment with only a slightly lower aspect ratio. Also all latest experiments with various aspect ratios do detect the wind of turbulence (see Belmonte *et al.* 1994; Xin *et al.* 1996; Qiu & Xia 1998; Lui & Xia 1998) whose existence we therefore consider as a weak – and in particular controllable – assumption. By the way, the direction of the wind may even vary over time.

The present theory does not make any statement about how the heat is transported from the bottom to the top, i.e. whether it is mainly convective transport or mainly transport through plumes as suggested by Belmonte *et al.* (1994) and by Ciliberto *et al.* (1996). Both processes may contribute, as both create thermal and viscous dissipation.

For even larger Prandtl numbers $Pr \gg 7$, the spontaneous formation of a wind of turbulence may seem more and more unlikely. To initiate such a wind so that this theory can be applied and results can be compared we suggest slightly tilting the RB cell, thus breaking the symmetry and creating a preferred direction for the wind of turbulence. If this wind can be created, we are confident that the suggested theory holds, but for further verification more experiments are required.

† For Pr of the order 1–10 the regimes $III_{u,l}$ are very small.

Note added in proof. In a very recent experiment by J. J. Niemela, L. Skrbek, K. R. Sreenivasan & R. J. Donelly ("Turbulent convection at very high Rayleigh numbers", preprint, 1999) the Nusselt number has been measured up to $Ra = 10^{17}$ and even beyond! A power-law exponent $\gamma = 0.309$ was determined. Fitting equation (3.1) in the Ra regime of 10^6 up to 10^{17} results in an effective exponent of 0.297, close to the experimental result. Ra and Pr are such that for large Ra regime IV_u is probed. Indeed, a linear plot of $Nu/(Ra^{1/4}Pr^{1/8})$ vs. $Ra^{1/12}Pr^{-1/8}$ gives a perfect straight line up to about $Ra = 10^{16}$, confirming the corresponding part of equation (3.3). Beyond $Ra = 10^{16}$, non-Boussinesq effects may play a role.

REFERENCES

ASHKENAZI, S. & STEINBERG, V. 1999 High Rayleigh number turbulent convection in a gas near the gas-liquid critical point. *Phys. Rev. Lett.* **83**, 3641–3644.

BELMONTE, A., TILGNER, A. & LIBCHABER, A. 1993 Boundary layer length scales in thermal turbulence. *Phys. Rev. Lett.* **70**, 4067–4070.

BELMONTE, A., TILGNER, A. & LIBCHABER, A. 1994 Temperature and velocity boundary layers in turbulent convection. *Phys. Rev. E* **50**, 269–279.

BENZI, R., TOSCHI, F. & TRIPICCIONE, R. 1998 On the heat transfer in the Rayleigh–Bénard system. *J. Statist. Phys.* **93**, 901–918.

BOBERG, L. & BROSA, U. 1988 Onset of turbulence in a pipe. *Z. Naturforsch.* **43a**, 697–726.

BUSSE, F. H. 1978 The optimum theory of turbulence. *Adv. Appl. Mech.* **18**, 77–121.

BUSSE, F. H. & CLEVER, R. M. 1981 An asymptotic model of two-dimensional convection in the limit of low Prandtl number. *J. Fluid Mech.* **102**, 75–83.

CASTAING, B., GUNARATNE, G., HESLOT, F., KADANOFF, L., LIBCHABER, A., THOMAE, S., WU, X. Z., ZALESKI, S. & ZANETTI, G. 1989 Scaling of hard thermal turbulence in Rayleigh–Bénard convection. *J. Fluid Mech.* **204**, 1–30.

CHAN, S. K. 1971 Infinite Prandtl number turbulent convection. *Stud. Appl. Maths* **50**, 13–49.

CHAVANNE, X., CHILLA, F., CASTAING, B., HEBRAL, B., CHABAUD, B. & CHAUSSY, J. 1997 Observation of the ultimate regime in Rayleigh–Bénard convection. *Phys. Rev. Lett.* **79**, 3648–3651.

CHILLA, F., CILIBERTO, S., INNOCENTI, C. & PAMPALONI, E. 1993 Boundary layer and scaling properties in turbulent thermal convection. *Il Nuovo Cimento* D **15**, 1229–1249.

CHING, E. S. C. 1997 Heat flux and shear rate in turbulent convection. *Phys. Rev. E* **55**, 1189–1192.

CILIBERTO, S., CIONI, S. & LAROCHE, C. 1996 Large-scale flow properties of turbulent thermal convection. *Phys. Rev. E* **54**, R5901–R5904.

CILIBERTO, S. & LAROCHE, C. 1999 Random roughness of boundary increases the turbulent convection scaling exponent. *Phys. Rev. Lett.* **82**, 3998–4001.

CIONI, S., CILIBERTO, S. & SOMMERIA, J. 1995 Temperature structure functions in turbulent convection at low Prandtl number. *Europhys. Lett.* **32**, 413–418.

CIONI, S., CILIBERTO, S. & SOMMERIA, J. 1997 Strongly turbulent Rayleigh–Bénard convection in mercury: comparison with results at moderate Prandtl number. *J. Fluid Mech.* **335**, 111–140.

CLEVER, R. M. & BUSSE, F. H. 1981 Low Prandtl number convection in a layer heated from below. *J. Fluid Mech.* **102**, 61–74.

CONSTANTIN, P. & DOERING, C. 1999 Infinite Prandtl number convection. *J. Statist. Phys.* **94**, 159–172.

DAVIS, A. H. 1922a Natural convective cooling of wires. *Phil. Mag.* **43**, 329–339.

DAVIS, A. H. 1922b Natural convective in cooling in fluids. *Phil. Mag.* **44**, 920–940.

DOERING, C. & CONSTANTIN, P. 1996 Variational bounds on energy dissipation in incompressible flows: III.: Convection. *Phys. Rev. E* **53**, 5957–5981.

DRAZIN, P. & REID, W. H. 1981 *Hydrodynamic Stability.* Cambridge University Press.

DU, Y. B. & TONG, P. 1998 Enhanced heat transport in turbulent convection over a rough surface. *Phys. Rev. Lett.* **81**, 987–990.

ECKHARDT, B. & MERSMANN, A. 1999 Transition to turbulence in shear flow. *Phys. Rev.* E **60**, 509–517.

FABER, T. E. 1995 *Fluid Dynamics for Physicists*. Cambridge University Press.

GARON, A. M. & GOLDSTEIN, R. J. 1973 Velocity and heat transfer measurements in thermal convection. *Phys. Fluids* **16**, 1818–1825.

GEBHARDT, T. & GROSSMANN, S. 1994 Chaos transition despite linear stability. *Phys. Rev.* E **50**, 3705–3711.

GLAZIER, J. A., SEGAWA, T., NAERT, A. & SANO, M. 1999 Evidence against ultrahard thermal turbulence at very high Rayleigh numbers. *Nature* **398**, 307–310.

GOLDSTEIN, R. J. & TOKUDA, S. 1980 Heat transfer by thermal convection at high Rayleigh numbers. *Intl J. Heat Mass Transfer* **23**, 738–740.

GROSSMANN, S. 1995 Asymptotic dissipation rate in turbulence. *Phys. Rev.* E **51**, 6275–6277.

GROSSMANN, S. 1999 The onset of shear flow turbulence. *Rev. Mod. Phys.*, in press.

HESLOT, F., CASTAING, B. & LIBCHABER, A. 1987 Transition to turbulence in helium gas. *Phys. Rev.* A **36**, 5870–5873.

HORANYI, S., KREBS, L. & MÜLLER, U. 1999 Turbulent Rayleigh–Bénard convection in low Prandtl number fluids. *Intl J. Heat Mass Transfer* **42**, 3983–4003.

HOWARD, L. N. 1972 Bounds on flow quantities. *Ann. Rev. Fluid. Mech.* **4**, 473–494.

KERR, R. 1996 Rayleigh number scaling in numerical convection. *J. Fluid Mech.* **310**, 139–179.

KRAICHNAN, R. H. 1962 Turbulent thermal convection at arbrtrary Prandtl number. *Phys. Fluids* **5**, 1374–1389.

KRISHNAMURTI, R. & HOWARD, L. N. 1981 Large scale flow generation in turbulent convection. *Proc. Natl Acad. Sci.* **78**, 1981–1985.

LANDAU, L. D. & LIFSHITZ, E. M. 1987 *Fluid Mechanics*. Pergamon.

LATHROP, D. P., FINEBERG, J. & SWINNEY, H. S. 1992 Turbulent flow between concentric rotating cylinders at large Reynolds numbers. *Phys. Rev. Lett.* **68**, 1515–1518.

LUI, S. L. & XIA, K. Q. 1998 Spatial structure of the thermal boundary layer in turbulent convection. *Phys. Rev.* E **57**, 5494–5503.

MALKUS, M. V. R. 1954 The heat transport and spectrum of thermal turbulence. *Proc. R. Soc. Lond.* A **225**, 196–212.

PROCACCIA, I., CHING, E. S. C., CONSTANTIN, P., KADANOFF, L. P., LIBCHABER, A. & WU, X. Z. 1991 Transition to convective turbulence: The role of thermal plumes. *Phys. Rev.* A **44**, 8091–8102.

QIU, X. L. & XIA, K.-Q. 1998 Viscous boundary layers at the sidewall of a convection cell. *Phys. Rev.* E **58**, 486–491.

ROBERTS, G. O. 1979 Fast viscous Bénard convection. *Geophys. Astrophys. Fluid Dyn.* **12**, 235–272.

ROSSBY, H. T. 1969 A study of Bénard convection with and without rotation. *J. Fluid Mech.* **36**, 309–335.

SCHMIEGEL, A. & ECKHARDT, B. 1997 Fractal stability border in plane Couette flow. *Phys. Rev. Lett.* **79**, 5250–5253.

SCHMIEGEL, A. & ECKHARDT, B. 1999 Dynamics of perturbations in plane Couette flow. Preprint, Marburg.

SHEN, Y., TONG, P. & XIA, K. Q. 1996 Turbulent convection over rough surfaces. *Phys. Rev. Lett.* **76**, 908–911.

SHRAIMAN, B. I. & SIGGIA, E. D. 1990 Heat transport in high-Rayleigh number convection. *Phys. Rev.* A **42**, 3650–3653.

SIGGIA, E. D. 1994 High Rayleigh number convection. *Ann. Rev. Fluid Mech.* **26**, 137–168.

SOLOMON, T. H. & GOLLUB, J. P. 1990 Sheared boundary layers in turbulent Rayleigh–Bénard convection. *Phys. Rev. Lett.* **64**, 2382–2385.

SPIEGEL, E. A. 1971 Convection in stars. *Ann. Rev. Astron. Astrophys.* **9**, 323–352.

TAKESHITA, T., SEGAWA, T., GLAZIER, J. A. & SANO, M. 1996 Thermal turbulence in mercury. *Phys. Rev. Lett.* **76**, 1465–1468.

TANAKA, H. & MIYATA, H. 1980 Turbulent natural convection in a horizontal water layer heated from below. *Intl J. Heat Mass Transfer* **23**, 1273–1281.

THRELFALL, D. C. 1975 Free convection in low temperature gaseous helium. *J. Fluid Mech.* **67**, 17–28.

TILGNER, A., BELMONTE, A. & LIBCHABER, A. 1993 Temperature and velocity profiles of turbulence convection in water. *Phys. Rev.* E **47**, R2253–R2256.

TREFETHEN, L., TREFETHEN, A., REDDY, S. & DRISCOL, T. 1993 Hydrodynamic stability without eigenvalues. *Science* **261**, 578–584.

VILLERMAUX, E. 1995 Memory-induced low frequency oscillations in closed convection boxes. *Phys. Rev. Lett.* **75**, 4618–4621.

WALEFFE, F. 1995 Transition in shear flows: Nonlinear normality versus non-normal linearity. *Phys. Fluids* **7**, 3060–3066.

WERNE, J. 1993 Structure of hard-turbulent convection in two-dimensions: Numerical evidence. *Phys. Rev.* E **48**, 1020–1035.

WU, X. Z. 1991 Along a road to developed turbulence: Free thermal convection in low temperature He gas. PhD thesis, University of Chicago.

WU, X. Z. & LIBCHABER, A. 1991 Non-Boussinesq effects in free thermal convection. *Phys. Rev.* A **43**, 2833–2839.

WU, X. Z. & LIBCHABER, A. 1992 Scaling relations in thermal turbulence: The aspect ratio dependence. *Phys. Rev.* A **45**, 842–845.

XIA, K.-Q. & LUI, S.-L. 1997 Turbulent thermal convection with an obstructed sidewall. *Phys. Rev. Lett.* **79**, 5006–5009.

XIN, Y. B. & XIA, K. Q. 1997 Boundary layer length scales in convective turbulence. *Phys. Rev.* E **56**, 3010–3015.

XIN, Y. B., XIA, K. Q. & TONG, P. 1996 Measured velocity boundary layers in turbulent convection. *Phys. Rev. Lett.* **77**, 1266–1269.

YAKHOT, V. 1992 4/5 Kolmogorov law for statistically staionary turbulence: application to high Rayleigh number Bénard convection. *Phys. Rev. Lett.* **69**, 769–771.

ZALESKI, S. 1998 The 2/7 law in turbulent thermal convection. In *Geophysical and Astrophysical Convection* (ed. P. Fox & R. Kerr). Gordon and Breach.

ZOCCHI, G., MOSES, E. & LIBCHABER, A. 1990 Coherent structures in turbulent convection: an experimental study. *Physica* A **166**, 387–407.